AFSC PROCESSED REPORT 2025-01

NOAA FISHERIES

Alaska Fisheries Science Center
Resource Assessment and Conservation Engineering Division
Groundfish Assessment Program

Results of the Acoustic-Trawl Survey of Walleye Pollock (*Gadus chalcogrammus*) on the U.S. Bering Sea Shelf in June - August 2022 (DY2207)

FEBRUARY 2025

U.S. Department of Commerce | National Oceanic and Atmospheric Administration | National Marine Fisheries Service

AFSC Processed Report

This document should be cited as follows:
Stienessen, S. C., McCarthy, A., Honkalehto, T., Lauffenburger, N., and Urmy, S. 2025. Results of the acoustic-trawl survey of walleye pollock (*Gadus chalcogrammus*) on the U.S. Bering Sea Shelf in June - August 2022 (DY2207). 2025. AFSC Processed Rep. 2025-01, 68 p. Alaska Fish. Sci. Cent., NOAA, Natl. Mar. Fish. Serv., 7600 Sand Point Way NE, Seattle WA 98115.

This document is available online at: https://repository.library.noaa.gov/

Results of the Acoustic-Trawl Survey of Walleye Pollock (*Gadus chalcogrammus*) on the U.S. Bering Sea Shelf in June - August 2022 (DY2207)

by

S. C. Stienessen, A. McCarthy, T. Honkalehto, N. Lauffenburger, and S. Urmy

Resource Assessment and Conservation Engineering Division
Alaska Fisheries Science Center
National Marine Fisheries Service
National Oceanic and Atmospheric Administration
7600 Sand Point Way, NE
Seattle, WA 98115

February 2025

ABSTRACT

Eastern Bering Sea shelf walleye pollock (*Gadus chalcogrammus*) midwater abundance and distribution were assessed from Bristol Bay to the U.S.-Russia Convention Line from 1 June to 5 August 2022 using acoustic-trawl (AT) survey methods aboard the NOAA ship *Oscar Dyson*. In addition to surveying the traditional survey area (core area), we also surveyed north of the standard endpoints along all transects that did not terminate at the U.S.-Russia Convention Line (northern extension) and completed two cross-shelf transects in the core area. Sea surface temperatures (SST) and bottom temperatures in the core area were cooler in 2022 (mean SST 7.1° C, mean bottom temperature 2.4° C) compared with temperatures during the previous AT surveys in 2016 and 2018 (mean SST 11.4° C and 8.5° C, respectively; bottom temperature 3.9° C and 3.7° C, respectively). The 2022 SST were still warmer than relatively cold conditions experienced during the 2006-2012 surveys (means between 4.9° C and 6.8° C); however, the 2022 bottom temperatures on the shelf north and west of the Pribilof Islands (range -1.5° C to 1.5° C) were characterstic of the 'cold pool' (< 2° C) . Walleye pollock biomass was concentrated between the 100 m contour and the shelf break, particularly north of Unimak Pass and between Zhemchug Canyon and the U.S.-Russia Convention line. The estimated amount of pollock in midwater (between 16 m from the sea surface and 0.5 m off the seafloor) in the core survey area was 9.67 billion fish with a biomass of 3.83 million metric tons (t), just over a 50% increase from the estimate of 5.57 billion fish with a biomass of 2.50 million t in 2018, the last time a standard acoustic-trawl survey was conducted on the eastern Bering Sea shelf. This year's estimated amount is also a 6% increase over the estimate of 3.62 million t in 2020 made by the acoustics-only Saildrone survey. Pollock east of 170° W numbered 2.99 billion fish and weighed 1.36 million t (36% of the total biomass found in the core survey area, and 31% of the biomass found shelf-wide, including the northern extension). Four year-old pollock (40 cm mean fork length (FL)) composed 59% of the biomass east of 170° W. Pollock abundance west of 170° W was 6.68 billion fish weighing 2.47 million t (64% of total core survey area biomass and 57% of the shelf-wide biomass, including the northern extension). Four year-old pollock (36 cm mean FL) composed 68% of the biomass west of 170° W. The mean biomass-weighted depth of adult pollock (≥ 30 cm FL, age-3+) was 95 m in the region east of 170° W and 86 m west of 170° W. Relatively few juveniles were observed east or west of 170° W.

The estimated amount of pollock in the northern extension was 76.6 million fish with a biomass of 0.54 million t (approximately 14% of the core survey area total).

CONTENTS

INTRODUCTION

Scientists from the Midwater Assessment and Conservation Engineering (MACE) Program of the Alaska Fisheries Science Center (AFSC) have conducted summer acoustic-trawl (AT) surveys to estimate the abundance and distribution of walleye pollock (*Gadus chalcogrammus*, hereafter "pollock") on the eastern Bering Sea (EBS) shelf since 1979. Surveys were conducted triennially through 1994 and have been conducted either annually or biennially since 1994. The surveys generally extend from seafloor depths of 50 m to 1,000 m, encompassing the middle (50 to 100 m isobaths) and outer (100 to 200 m isobaths) domains of the Bering Sea shelf. The 2022 AT survey was carried out between 2 June and 5 August aboard the NOAA ship *Oscar Dyson*. The primary objective was to estimate pollock midwater abundance and distribution within the U.S. portion of the Bering Sea shelf using AT survey methods. Due to a delayed departure and uncertainty about survey completion caused by vessel crew shortages, the survey was conducted at a lower resolution (i.e., increased transect spacing, less trawling) than in the past. This resulted in the traditional (core) area being surveyed over 2 legs versus the standard 3 legs. Leg 3 ultimately occurred, and during that time surveys of the inshore areas in the southeast and areas north of St. Matthew Island (collectively, 'the northern extension') were conducted to investigate presence of age-1+ pollock outside the core area, and cross-shelf transects in the core area were surveyed to examine spatial variability due to increased transect spacing. The adjoining Russian portion of the EBS shelf was not surveyed as we revoked our application to survey in Russian waters in March, and permission to survey that region was not granted in 2022. Additional sampling included conductivity-temperature-depth (CTD) probes to characterize shelf oceanographic conditions.

Here we report estimates of pollock abundance and biomass by size and age from near the sea surface to 0.5 m off the seafloor. Other survey results presented include 1) acoustic system calibration, 2) physical oceanographic (temperature) spatial patterns, 3) pollock biomass spatial patterns, 4) spatial patterns of non-pollock backscatter, 5) pollock biomass-weighted vertical distributions, 6) AT survey time series of pollock abundance estimates, and 7) the results of the cross-shelf transect spatial variability.

METHODS

All activities were conducted aboard the NOAA ship *Oscar Dyson*, a 64-m stern trawler equipped for fisheries and oceanographic research. The survey followed established AT methods as specified in NOAA protocols for fisheries acoustics surveys and related sampling[1]. The acoustic units used here are defined in MacLennan et al. (2002). Survey itineraries are listed in Appendix I and scientific personnel in Appendix II.

Acoustic Equipment, Calibration, and Data Collection

Acoustic measurements were collected with a Simrad EK80 scientific echosounder (Bodholt and Solli 1992, Simrad 2018). Data were collected with five split-beam transducers (18, 38, 70, 120, and 200 kHz) mounted on the bottom of the vessel's retractable centerboard, which was extended 9.15 m below the water surface.

Standard sphere acoustic system calibrations were conducted to measure acoustic system performance (Table 1). The vessel's dynamic positioning system was used to maintain the vessel location during calibration. Local water temperature and salinity were measured and used to estimate absorption and sound speed. A tungsten carbide sphere (38.1 mm diameter) suspended below the centerboard-mounted transducers was used to calibrate the 38, 70, 120, and 200 kHz systems. The tungsten carbide sphere was then replaced with a 64 mm diameter copper sphere to calibrate the 18 kHz system. A two-stage calibration approach was followed for each frequency. On-axis sensitivity (i.e., transducer gain and s_A correction) was estimated from measurements with the sphere placed in the center of the beam following the procedure described in Foote et al. (1987). Transducer beam characteristics (i.e., beam angles and angle offsets) were estimated by moving the sphere in a horizontal plane using the EK80's calibration utility (Jech et al. 2005, Simrad 2018). The equivalent beam angle (for characterizing the volume sampled by the beam) and angle sensitivities (for conversion of electrical to mechanical angles) cannot be estimated from the calibration approach used because that requires knowledge of the absolute position of the sphere (see Demer et al. 2015). Therefore, the factory default

[1] National Marine Fisheries Service (NMFS) 2014. NOAA protocols for fisheries acoustics surveys and related sampling (Alaska Fisheries Science Center), 26 p. Prepared by Midwater Assessment and Conservation Engineering Program, Alaska Fish. Sci. Center, Natl. Mar. Fish. Serv., NOAA.

values for equivalent beam angle and angle sensitivities for each transducer were used during calibration.

Raw acoustic data were recorded using EK80 software (version 2.0.1 for Legs 1-2, version 21.15.1 for Leg 3) at a nominal ping interval of 1.2 seconds, and analyzed from 16 m below the sea surface to within 0.5 m of the sounder-detected bottom to a maximum depth of 1,000 m. Data shallower than 16 m were excluded to account for the acoustic near-field range of all transducers (Simmonds and MacLennan 2005). Data within 0.5 m of the seafloor were also excluded to account for the bottom-associated acoustic dead zone (Ona and Mitson 1996). The raw acoustic data were analyzed using Echoview post-processing software (version 12.1.27, Echoview Software Pty Ltd).

Trawl Gear and Oceanographic Equipment

Midwater acoustic backscatter (defined as 16 m from the surface to 3 m off bottom) was sampled using an LFS1421 trawl[2]. The headrope and footrope of the LFS1421 trawl each measure 76.8 m (252 ft), with meshes tapering from 650 cm (256 in.) in the forward sections to 3.8 cm (1.5 in.) in the section immediately preceding the codend. The codend was made of 8.9 cm (3.5 in.) mesh (mesh sizes are stretched measurements unless otherwise noted). To increase retention of small organisms, the LFS1421 codend is fitted with a knotless nylon 7.9 mm (5/16 in.) mesh, 3.2 mm (1/8 in.) square-opening codend liner. Midwater backscatter was occasionally sampled with an 83-112 Eastern bottom trawl without roller gear constructed with mesh sizes that range from 10.2 cm (4.0 in.) in the forward portion of the net to 8.9 cm (3.5 in.) in the codend and fitted with a heavy delta nylon 12.7 mm (1/2 in.) mesh, 6.4 mm (1/4 in.) square opening codend liner. Detailed specifications are described in Honkalehto et al. (2002). Near-bottom backscatter (between 3 m and 0.5 m off bottom) was sampled using 83-112 Eastern bottom trawls (with the same characteristics as above) with hauls made on a regular 20 × 20 nmi grid during the 2022 EBS bottom trawl (BT) survey carried out between 30 May and 29 July as described in Markowitz et al. (2023).

[2] LFS1421 trawl (LFS Marine, NOAA, 1421 Research Trawl, designed and built in 2018/2019 to MACE specifications; hereafter LFS1421).

The LFS1421 trawl was fished with four 45.7 m (150 ft) bridles (1.9 cm (0.75 in.) dia.), 5 m^2 Fishbuster trawl doors (1,247 kg (2,750 lb) each), and 227 kg (500 lb) tom weights attached to each wingtip. Average trawling speed was 1.8 m s^{-1} (3.4 knots). LFS1421 trawl vertical net openings and headrope depths were monitored with a Simrad FS70 third-wire netsonde attached to the headrope. The vertical net opening of the LFS1421 trawl ranged from 12.0 to 34.3 m (39.4 to 112.6 ft) and averaged 17.5 m (57.3 ft) while fishing. Average trawling speed for the AT survey 83-112 was 1.7 m s^{-1} (3.3 knots), and vertical net openings and seafloor contact were monitored with a Furuno CN-24 netsounder system mounted on the headrope. The vertical net opening of the AT survey 83-112 averaged 3.0 m (9.8 ft). See Markowitz et al. (2023) for the BT survey 83-112 trawl details.

A Methot trawl (Methot 1986) was used to target midwater acoustic layers containing macro-zooplankton such as euphausiids, age-0 pollock, and other larval fishes. The Methot trawl had a rigid square frame measuring 2.3 m (7.5 ft) on each side, which formed the mouth of the net. The body of the net consisted of nylon 63.5 mm (2.5 in.) mesh material, lined with delta nylon 1/8 in. mesh material with 2 mm × 3 mm oval openings, and attached to a hard plastic codend bucket lined with 1 mm × 1 mm square opening mesh. A 1.8 m (5.9 ft) dihedral depressor was used to generate additional downward force. A calibrated General Oceanics flowmeter was attached to the mouth of the net; the number of flowmeter revolutions and the total time the net was in the water were used to determine the volume of water filtered during the haul. The Methot trawl was attached to a single cable fed through a stern-mounted A-frame. Real-time haul depths were monitored using a Simrad ITI acoustic link temperature-depth sensor attached to the bottom of the Methot frame. The Methot trawl was towed at an average speed of 1.5 m s^{-1} (2.8 knots). Although catch composition from the Methot trawls is reported here (see Table 8), the abundance and biomass estimates of euphausiids, derived in part from the Methot catch data, are reported elsewhere (Ressler 2022).

To estimate escapement of smaller fishes from the net, recapture (or pocket) nets were placed at several locations along the LFS1421 net (Williams et al. 2011, Honkalehto et al. 2022). The LFS1421 trawl was fitted with a total of nine recapture nets placed on forward (813 mm mesh), mid (102 mm mesh), and aft (102 mm mesh) sections of the trawl, with one recapture net attached on the top, bottom, and port panel of each section. The recapture nets were constructed

from knotless nylon 7.9 mm (5/16 in.) mesh, 3.2 mm (1/8 in.) square-opening mesh material (matching the codend liner).

A stereo camera system (Camtrawl; Williams et al. 2010) was attached to the starboard panel forward of the codend on the LFS1421 trawl. The Camtrawl is used to capture stereo images for species identification and length measurement of individual fish and other taxa as they pass through the net toward the codend. The Camtrawl data are useful for determining the depth and size distribution of fish and other taxa when distinct and separate backscatter layers are sampled by a trawl haul but cannot be differentiated in the codend catch. Images were viewed and annotated using procedures described in Williams et al. (2010).

Physical oceanographic data collected during the cruise included temperature profiles obtained with a temperature-depth probe (SBE 39, Sea-Bird Scientific) attached to the trawl headrope. Additional temperature-depth measurements were taken from conductivity-temperature-depth (CTD) casts with a Sea-Bird CTD (SBE 911plus) system at calibration sites and throughout the survey to describe EBS shelf temperature features associated with pollock and euphausiids. CTD casts were made at the closest point along a survey transect to 16 set stations located in the core area and 4 set stations located in the northern extension, selected to provide a systematic, representative set of water column observations (P. Stabeno, PMEL, pers. commun.) to complement SBE profiles. Additional CTD casts usually made near the location where daylight transect operations ended each day were not conducted in 2022 due to vessel crew limitations. This sampling strategy is typically repeatable each survey year with minimal impact on other survey operations. Salinity bottle samples (e.g., one bottle every other day, alternating at surface and bottom of cast) were collected from the casts to calibrate the CTD conductivity sensor. Sea surface temperature data were measured using the ship's sea surface temperature system (SBE 38, Sea-Bird Scientific, accuracy $\pm$ 0.002°C) located near the ship's bow, approximately 1.4 m below the surface. At times when the SBE 38 was not operating, sea surface temperatures were taken from the Furuno T-2000 temperature probe (accuracy $\pm$ 0.2°C) located amidships 1.4 m below the surface. The SBE 38 was used 89.5% of the time in the eastern Bering Sea survey. These and other environmental data were recorded using the ship's Scientific Computing Systems (SCS).

Survey Design

The 2022 survey design consisted of a series of parallel transects spaced 74 km (40 nmi) apart. Traditionally, this survey consists of parallel transects spaced 37 km (20 nmi) apart and is conducted over three ca. 3-week long legs. However, when the survey began it was unclear whether the *Oscar Dyson* would be able to crew all three legs. Sailing delays on each leg due to the COVID-19 pandemic were also possible. It was therefore decided to reduce transect spacing from 37 km to 74 km spacing to allow for completion of the standard survey area in the EBS (i.e., "core area"; Fig. 1) within 2 abbreviated legs. This modified survey design resulted in 14 parallel transects planned over the core area. It also represents half the sampling density of surveys conducted prior to 2020 (transects 37 km apart), but it is equal to the sampling density of the 2020 survey (De Robertis et al. 2021). Near the end of Leg 2, there was enough time remaining to increase sampling density. The NW region of the core area was thus sampled at 37 km transect spacing, resulting in a total of 16 parallel transects conducted over the core area (Fig. 1). Transect start and end locations in the core area matched those from previous surveys and extended from water depths of ~60-80 m to the shelf break (> 1,000 m). Leg 3 did occur and investigated the presence of age-1+ pollock north of the core area (e.g., "northern extension"). This was done by extending the eastern 11 core transects (i.e., those transects whose northern terminus did not end at the U.S.-Russia Convention line) northward to water depths of ~40-50 m, spaced at 74 km apart (Fig. 1). The survey of both the core area and northern extension was conducted during daylight hours (e.g., ~18 hours a day). Upon completion of the northern extension, two cross-shelf transects were surveyed en route back to port to evaluate the scale of spatial autocorrelation in the observations (Fig. 1).

The AT survey trawl hauls were conducted to identify the species and size composition of acoustically-observed fish aggregations and to determine biological characteristics of pollock and other specimens. Trawl hauls are normally conducted opportunistically during survey hours. This is roughly 18 daylight hours per day, approximately 0600 to 0000 AST; however, due to crew shortages on the *Oscar Dyson*, trawl hauls were only conducted during a 12-hour window in 2022, between 0900 and 2100. Catches were sorted to species and weighed. When large numbers of juvenile and adult pollock were encountered, the predominant size groups in the catch were sampled separately (e.g., age-1 vs. larger sizes). Fork length (FL), body weight, sex (FL > 20 cm), maturity, age (otoliths), and gonad measurements were collected for a random

subset of pollock within each size group. Pollock and other fishes were measured to the nearest 1 mm FL, or standard length (SL) for small specimens, with an electronic measuring board (Towler and Williams 2010). All lengths measured as SL were converted to FL using an SL to FL regression obtained from historic survey data. Gonad maturity was determined by visual inspection and categorized as immature, developing, mature (hereafter, "pre-spawning"), spawning, or spent[3]. The ovary weight was determined for pre-spawning females. An electronic motion-compensating scale (Marel M60) was used to weigh individual pollock and selected ovaries to the nearest 2 g. Otoliths that were collected were stored in 50% glycerin/thymol/water solution and interpreted by AFSC Age and Growth Program researchers to determine fish ages. Trawl station information and biological measurements were electronically recorded using the MACE Program's custom Catch Logger for Acoustic Midwater Surveys (CLAMS) software. Catch processing and sampling procedures from the 30 minute 83-112 bottom trawls conducted during the 2022 EBS bottom trawl survey are given by Markowitz et al. (2023). Briefly, total numbers and weights by species were either fully measured or expanded from subsamples when the total catch was > 1,200 kg. A subsample of up to 100 individuals of select species, based on the range of sizes of that species within the haul, were sexed, lengthed, and indivudally weighed. Otolith samples of some of those individuals were collected based on random-by-haul sampling methods, stored in 50% glycerin/thymol/water solution, and also interpreted by AFSC Age and Growth Program researchers to determine fish ages.

Further biological samples were collected for special projects. Pollock ovaries were collected from pre-spawning pollock to investigate interannual variation in fecundity of mature females (Sandi Neidetcher, Sandi.Neidetcher@noaa.gov), and from female pollock of all maturity stages for a histological study. Fin clips were taken from pollock to investigate the genetic population structure within spawning stocks (Ingrid Spies, Ingrid.Spies@noaa.gov), and gill tissues from pollock and Pacific cod (*Gadus microcephalus*) were collected for an evolutionary marker analysis (Einar Arnason, Univeristy of Iceland, einararn@hi.is). Blood and tissue samples were also taken from pollock and cod to investigate the prevalence of antifreeze proteins (Chi-Hing Christina Cheng, Univeristy of Illinois Urbana-Champaign, c-cheng@illinois.edu). Whole

[3] Groundfish Survey and Species Codes. 2019. RACE Division, AFSC, NMFS, NOAA; 7600 Sand Point Way NE, Seattle, WA 98115. Available online: https://www.fisheries.noaa.gov/resource/document/groundfish-survey-species-code-manual-and-data-codes-manual.

Pacific herring (*Clupea pallasii*) were collected for a genetic diversity study and population structure analysis (Savannah LaBua, Florida International University, slabu003@fiu.edu).

Additonally, two moorings were deployed, and one moorning was recovered, during the survey. These moorings were used to track the timing and occurrence of marine mammal species in the Bering Sea and to monitor changes in their acoustic environment (Catherine Berchok, Catherine.Berchok@noaa.gov).

Data Analysis

Pollock abundance was estimated by combining acoustic and trawl catch information. The analysis method employed here for midwater estimates between 16 m from the surface and 3 m off bottom had three principal steps. First, backscatter was associated with the trawl catches from the nearest geographic haul locations within a stratum. Second, a correction was made for net selectivity (escapement from the midwater net, based on relationships derived from recapture nets; Williams et al. 2011). Third, backscatter was converted to estimates of abundance using the nearest-haul catch association (step 1) with sample corrections (step 2) and the expected backscatter from each organism given species and size. Biomass was computed from abundance using the mean weight-at-length from all pollock specimens measured in the survey.

The analysis employed to compute near-bottom estimates between 0.5 and 3 m off bottom followed a similar path (described more completely below), though the backscatter was associated with the nearest bottom trawl catch from the separate BT survey (Markowitz et al. 2023), no selectivity was applied to the bottom trawl catch, and a relationship by species was used to scale the near-bottom contribution following Lauffenburger et al. (2017). The abundance and biomass estimates from the midwater and near-bottom were combined to generate final values from 16 m from the surface to 0.5 m off the seafloor.

Processing of Acoustic Data

Although acoustic data were recorded at five frequencies, the results of this report and the survey time series are based on the 38 kHz data. The sounder-detected bottom was calculated by averaging the bottom detections for all five frequencies (Jones et al. 2011) and then visually

examined to remove any bottom integrations. A minimum S_v threshold of –70 dB re 1 m^{-1} was applied to the 38 kHz acoustic data, which were then echo-integrated from 16 m below the surface to 0.5 m above the sounder-detected bottom. Data were averaged at 0.5 nmi horizontal by 10 m vertical resolution intervals and exported to a database.

Associating Size and Species Composition with Midwater Acoustic Backscatter

Acoustic backscatter was assigned to strata based on the appearance and vertical distribution of the aggregations in the echogram between 16 m from the surface to 3 m off the seafloor. Strata containing backscatter not considered to be from pollock (e.g., the near-surface mixture of unidentifiable backscatter, backscatter with frequency response indicative of euphausiids or myctophids (De Robertis et al. 2010), or near-bottom backscatter "haystack" morphology indicative of some rockfishes) were excluded from further analyses. Each trawl was associated with a stratum, and the midwater backscatter at a given location was associated with the species and size composition of the geographically-nearest haul within that stratum (see De Robertis et al. 2017b for details). For example, juvenile pollock can be found in shallow, dense schools with a diffuse layer of adult pollock at deeper depths in the same area. In this case, the backscatter dominated by aggregations of juveniles would be assigned to a shallow stratum (A) and the backscatter dominated by adult layers would be assigned to a deep stratum (B). Hauls that sampled the shallow layer would be assigned to stratum A, and hauls that sampled the deeper layer would be assigned to stratum B. Midwater backscatter was apportioned by species and size within a stratum using the selectivity-corrected catch composition from the geographically-nearest trawl in that stratum and converted to abundance.

Accounsting for Catch from Non-Targeted Midwater Scattering Layers

As noted above, each trawl was associated with an acoustic stratum. However, trawls may capture animals while passing through non-targeted strata during the trawling process. For example, a trawl targeting a deep stratum may capture acoustically-relevant animals while passing through a shallower stratum during set and retrieval. Because trawls aggregate catch from all the strata sampled, animals from the shallow stratum could then be associated incorrectly with the deeper stratum during analysis. These animals should not be included in the catch that is applied to the deeper stratum.

To avoid incorrectly applying catch from different strata, Camtrawl images collected during LFS1421 trawls were used to identify catch depth and location in the water column. Camtrawl images were captured at a rate of approximately 1 s^{-1} and each image was tagged with collection time and depth. Analysts visually identified and counted animals present in every 100^{th} image (approximately one image per 1.5 minute of trawl time) using SEBASTES Stereo Image Analysis software (Williams et al. 2016). For every examined image, the analyst identified all visible fish to the lowest taxonomic level possible, and identified invertebrates to broad taxonomic group (i.e., 'jellyfish', 'squid', 'shrimp'). Images were then examined using custom Python applications to identify cases where the trawl retained catch from non-targeted layers. In rare, exceptional cases where it was evident that the trawl catch contained acoustically-relevant species and/or size classes from outside of the target stratum, these species and/or size class records were excluded during the analysis process from the trawl catch associated with the target stratum (see Figs. 3 and 4 in Levine et al. (2024) for a summary of the review process).

Selectivity Correction

Previous research has found that smaller pollock are less likely to be retained in large midwater trawls than larger pollock (Williams et al. 2011). To correct for species- and size-related differences in retention, trawl catch compositions were adjusted to that which would be expected from an unselective net. Trawl selectivity for all species in the 2022 survey was estimated using correction functions developed from catch data collected by recapture nets mounted on the LFS1421 trawl in the 2019 summer Gulf of Alaska survey (Jones et al. 2022), although due to lack of small fish in the trawl samples, the selectivity correction for 2022 is likely negligible. No selectivity correction has been estimated for the bottom trawls used in this survey. The counts and weights of fish and other taxa caught in the recapture nets were expanded to provide an estimate of escapement from the entire trawl. The catch of all species was corrected for the estimated probability of escapement by dividing the abundance of a given species and size class by the estimated probability of retention of that species and size class. The probability of retention was calculated using either species-specific trawl selectivity correction functions for the most abundant species or more generic selectivity functions for less abundant species that were pooled together (Honkalehto et al. 2022, De Robertis et al. 2017b). Thus, the 2022 survey estimates reflect adjustments to the trawl-derived estimates of species and size composition which incorporate the estimated escapement of all organisms from the catch (e.g., De Robertis et al. 2017a).

Abundance Calculations

A series of target strength (TS, dB re 1 m^2; the expected backscatter from each organism) to length relationships from the literature (Table 2) were used along with size and species distributions from trawl catches to estimate the proportion of the observed acoustic scattering attributable to each of the species captured in the trawls (Appendix III). For species for which the TS to length relationship was derived using a different length measurement type than the one used for measuring the trawl catch specimens, an appropriate length conversion was applied. The most appropriate TS to length relationship available in the literature was used for each species or species group (Table 2). Taxa for which a more specific TS to length relationship was not available in the literature were assigned one of five TS-length relationship groups: fishes with swim bladders, fishes without swim bladders, jellyfish, squid, and pelagic crustaceans (Table 2).

Biomass was computed from abundance using the mean weight-at-length from all pollock specimens included in the length-weight key, which in summer 2022 was specimens lengthed and weighed in all survey trawl catches targeting pollock. When < 5 pollock occurred within a 1-cm length interval, weight at a given length interval was estimated from a linear regression of the natural logs of the length and weight data and corrected for a small bias due to back-transformation (Appendix III; Miller 1984, De Robertis and Williams 2008).

Four age-length keys and one proportion-at-age matrix were applied to the population numbers-at-length and biomass-at-length to estimate numbers and biomass-at-age (Appendix III; Jones et al. 2019). Historically pollock length-at-age tended to be greater in the east than the west, even though data were collected up to 6 weeks earlier east of 170° W. Therefore, two age-length keys were applied to the core area: all survey trawl catches targeting pollock in 1) the core area east of 170º W were used in estimations for the core area east of 170º W, 2) the core area west of 170º W were used in estimations for the core area west of 170º W. Additionally, another two age-length keys were applied to the northern extension: all survey trawl catches targeting pollock in 3) the core area and northern extension east of 170º W were used in estimations for the northern extension east of 170º W, and 4) the core area and northern extension west of 170° W were used in estimations for the northern extension west of 170º W. For population estimates-at-lengths where no otolith specimens were collected, the proportion-at-age was

estimated using a Gaussian-model approach based on historical age-at-length data (2000-2014; Jones et al. 2019).

Processing of Maturity Data

Maturity data for each haul in the AT survey were weighted by the local acoustically-estimated abundance of adult pollock (number of individuals > 30 cm FL) between 16 m from the surface and 0.5 m off bottom. The 30 cm size criterion was selected as the approximate minimum size at which historically ≥ 5% of pollock are mature. The sum of the local acoustically-estimated abundance assigned to the geographically-nearest haul, A_h, was computed. A weight was then assigned to each haul, W_h, by dividing A_h by the average acoustically-estimated abundance per haul $\overline{A}$,

$$W_h = \frac{A_h}{\overline{A}}\ , \qquad \text{(Eq. 1)}$$

where

$$\overline{A} = \frac{\sum_h A_h}{H}, \qquad \text{(Eq. 2)}$$

and H is the total number of hauls.

The percent of pollock, $PP_{sex,mat}$ > 34 cm FL by sex and maturity stage (immature, developing, pre-spawning, spawning, or spent) was computed for each haul and combined by survey area using a weighted average with W_h,

$$PP_{sex,mat} = \frac{\sum_h \left(N_{sex,mat,h} \cdot W_h\right)}{\sum_h W_h}, \qquad \text{(Eq. 3)}$$

where $N_{(sex,mat,h)}$ is the number of pollock > 34 cm FL by sex and maturity for each haul. The > 34 cm cutoff is used for consistency with reporting from past summer EBS surveys.

Near-bottom Analysis

Historically, AT survey results on the U.S. EBS shelf were presented for the water column between 16 m and 3 m off the seafloor. The analysis did not extend deeper than 3 m above the seafloor because 1) diverse catches in bottom trawl survey suggested that pollock may not dominate the backscatter close to the seafloor, and 2) the annual bottom trawl (BT) survey samples to a nominal depth of 2.5-3.0 m above the seafloor in the U.S. EEZ (Markowitz

et al. 2023). An approach was developed (Lauffenburger et al. 2017) to estimate the acoustic contribution of pollock relative to other species in the diverse region between 0.5 and 3 m off bottom using a combination of AT and BT data and first applied to EBS survey results in 2016 (Honkalehto et al. 2018).

Each 0.5 nmi interval of near-bottom backscatter between 3 m and 0.5 m off bottom was associated with BT trawls within 25 nmi. No selectivity corrections were applied to the BT trawls. The backscatter was scaled using a distance-weighted scaling of these selected trawls and the species-specific parameters derived in Lauffenburger et al. (2017) that describe the relative contribution of near-bottom fish species to this near-bottom backscatter. Abundance and biomass by length and age are computed in a similar fashion as described above for the midwater, except here the length-weight and age-length relationships are determined by the collective BT trawl data. Full water column results are reported here as the sum of the results from the midwater and near-bottom portions (16 m from the surface down to 0.5 m off bottom).

Relative Estimation Error

Transects were parallel and relative estimation errors for the acoustic-based estimates between 16 m from the surface to 0.5 off bottom were derived using a one-dimensional (1-D) geostatistical method (Petitgas 1993, Williamson and Traynor 1996, Walline 2007). "Relative estimation error" is defined as the ratio of the square root of the 1-D estimation variance ($variance_{sum}$) to the biomass estimate (i.e., the sum of biomass over all transects, $biomass_{sum}$, kg):

$$Relative\ estimation\ error_{1-D} = \frac{\sqrt{variance_{sum}}}{biomass_{sum}} \ . \qquad \text{(Eq. 5)}$$

Estimation variance was determined separately for the core area and northern extension.

Geostatistical methods were used to compute estimation error to account for estimation uncertainty arising from the observed spatial structure in the fish distribution. These errors, however, quantify only across-shelf transect sampling variability of the acoustic data (Rivoirard et al. 2000). Other sources of error (e.g., target strength, trawl sampling) were not evaluated.

Additional Analyses

Pollock vertical distribution patterns were computed by plotting the mean biomass in each 10 m depth bin, at the midpoint of each bin, relative to the surface (i.e., mean weighted depth, MWD) and to the seafloor (i.e., height above bottom, HAB). The MWD in each along-track interval *i* is computed as:

$$MWD_i = \sum_j \left(\left(\frac{B_{i,j}}{\sum_j B_{i,j}} \right) d_{i,j} \right), \qquad \text{(Eq. 6)}$$

where $B_{i,j}$ is observed biomass in 0.5 nmi along-track interval i and 10 m depth bin j, and d is the depth in meters of bin i from the sea surface. The HAB is computed in a similar fashion:

$$HAB_i = \sum_j \left(\left(\frac{B_{i,j}}{\sum_j B_{i,j}} \right) h_{i,j} \right), \qquad \text{(Eq. 7)}$$

where the terms are as described above and h is the height in meters of bin i above the sounder-detected bottom. MWD and HAB were summarized for a given survey area by first summing biomass over all intervals i in the area and then computing the MWD and HAB using the equations above.

Cross-Shelf Transect Spatial Analysis

Pollock biomass (in kg nmi^{-2}) was calculated in each 0.5 nmi horizontal distance of the longer cross-shelf transect between 16 m from the surface and 0.5 m off bottom using only trawl data collected on the acoustic survey. Anisotropy in spatial autocorrelation was analyzed by comparing three empirical variograms, which are functions (γ) giving the average variance (plotted by convention as half the average variance, or semivariance) between samples at a given separation or lag (Rivoirard et al. 2000). The first was calculated in the north-south direction, using only the standard north-south transects. The second was calculated using only the longer 144° cross-shelf transect. The third was an omnidirectional, isotropic variogram using the north-south transects and 144° cross-shelf transect. Prior to calculating these empirical variograms, the biomass values were transformed to approximately follow a standard normal distribution using a non-parametric transform based on their empirical cumulative distribution (Walline 2007). All three variograms were calculated for lags from 0- 200 km (0-108 nmi), in bins 4 km (2.2 nmi) wide. An exponential model was fitted to each of these empirical variograms, with the data weighted inverse to the lag distance to ensure a good fit at short lags (Rivoirard et al. 2000). The biomass density along each of the 16 north-south transects, also

collected between 16 m from the surface and 0.5 m off bottom using only trawl data collected on the acoustic survey, was summed to obtain a 1D series. Sixteen data points are not enough to reliably calculate a variogram, but transect averages were tested for evidence of spatial autocorrelation using the Ljung-Box *Q* statistic for up to four lags (Ljung and Box 1978).

RESULTS AND DISCUSSION

Calibration

Initial acoustic system settings for the survey were based on results from the 31 May calibration (Table 1). The middle and end-of-cruise 38 kHz calibrations on 9 July and 5 Aug. exhibited a small difference (-0.07 dB and 0.10 dB, respectively) from the initial calibration on-axis sensitivity gain result (Table 1). Both values are smaller than the discrepancy typically observed on most surveys (< 0.2 dB). There was no evidence of equipment malfunction during this survey. Acoustic data were thus processed using an average of the pre-, mid-, and post-cruise (linearized) gain values. Using the average of all calibrations resulted in a 1.5% increase in backscatter values compared to values extracted with the pre-cruise gain.

Water Temperature

The mean sea surface temperature (SST) during the 2022 survey of the core area was 7.1° C (range 3.4°-9.0° C; Fig. 2a). This was cooler than 2018 (mean SST 8.5° C, range 5.2°-10.6° C) and 2016 (mean SST 11.4° C , range 7.4°-14.0° C), but still warmer than relatively cold conditions experienced during the 2006-2012 surveys (means between 4.9°-6.8° C). Seasonal warming of surface waters typically leads to maximum SST in August (Overland et al. 1999), and the warmest SSTs observed in the 2022 EBS survey were during the cross-shelf transect through the core area in early August (mean 9.3° C, max 10.1° C). SSTs were coolest between the Pribilof Islands and St. Matthew Island in mid-to-late June. Bottom temperatures in 2022 from CTD casts (mean 2.4° C in the core area, mean 1.2° C in the northern extension, Fig. 2b) were lower than all recent years, and more characteristic of the 'cold pool' (< 2.0° C, Wyllie-Echeverria and Wooster 1998). Temperature-depth profiles from trawl headrope sensors indicate that the water column was vertically stratified with a thermocline at roughly 15-25 m from the surface (Fig. 3). The EBS shelf region west of 170° W was somewhat more vertically stratified than east of 170° W, and the northern extension was more stratified than the core area (Fig. 3). Trawl headrope temperatures below the thermocline were slightly warmer on average east of 170° W (> 3° C) than west of 170° W (≤ 3° C). Trawl headrope temperatures below the thermocline in the northern extention were

markedly cooler (< 0° C) and more similar to headrope temperatures observed in the core area during recent cold years (2007-2012).

Trawl Sampling

Biological data and specimens applied to the midwater backscatter observed between the near-surface and 3 m off bottom were collected during the AT survey from 48 trawl hauls in the core area, and 18 trawl hauls in the northern extension (Table 3, Fig. 1). All of these hauls targeted backscatter during daytime for species classification during the survey: in the the core area and northern extension 43 and 16 hauls, respectively, were conducted with a LFS, 2 and 1 hauls, respectively, with a AT survey 83-112, and 3 and 1 hauls, respectively, with a Methot trawl. An additional 9 trawl hauls (8 LFS and 1 Methot) were collected on the cross transect survey (Table 3, Fig. 1). Catch data from the core area and northern extension are presented by LFS and AT survey 83-112 net type in Tables 4-7. Catch data from all Methot trawls are presented in Table 8. Biological data and specimens applied to the near-bottom backscatter (0.5 m off bottom - 3 m off bottom) were from 376 BT survey 83-112 hauls conducted in the core area and 144 ST survey 83-112 hauls conducted in the northern extension (Markowitz et al. 2023).

Age-1+ pollock (hereafter "pollock" refers to age-1+ pollock) was the most abundant species in LFS midwater haul catches in the core area by weight (89.0%) and by number (93.8%), followed by Pacific ocean perch (*Sebastes alutus*; 5.4% by weight and 2.4% by number) and northern sea nettle jellyfish (*Chrysaora melanaster*; 5.2% by weight and 3.2% by number, Table 4). Among AT survey 83-112 hauls done in the core area, pollock was the most abundant species by weight (82.9%) and by number (89.3%), followed by northern sea nettle jellyfish (9.8% by weight and 3.8% by number, Table 5). Pollock also contributed 37% by weight to the BT survey catches based on the 83-112 hauls done within the core area (Markowitz et al. 2023).

Pollock was the most abundant species in LFS midwater haul catches in the northern extension by weight (48.4%) followed by northern sea nettle jellyfish (25.4%), but age-0 pollock was the most abundant organism by number (99.7%, Table 6). In the AT survey 83-112 hauls done in the northern extension, yellowfin sole (*Limanda aspera*) was the most abundant species by weight (9.9%) followed by pollock (4.1%), but again, age-0 pollock was the most abundant organism by number (93.1%, Table 7). Pollock also contributed 24% by weight to the BT survey catches based on the 83-112 hauls done within the northern extension (Markowitz et al. 2023).

Throughout the entire survey region (core area, northern extension, and cross transect), northern sea nettle was the most abundant species by weight in Methot hauls (89.8%), followed by euphausiids (5.8%, Table 8). Euphausiids were the most abundant species by number (96.7%), followed by unidentified jellyfish (2.2%).

A little over 17,000 lengths were measured and 3,100 specimen weights were collected for all species during the LFS and 83-112 hauls conducted in the core area during the AT survey (Tables 4 and 5). Of those, a little less than 16,000 lengths, 2,500 weights, and 2,100 otoliths were pollock (Table 9). A little over 2,100 lengths were measured and 700 specimen weights were collected for all species during the LFS and AT survey 83-112 hauls conducted in the northern extension (Tables 6 and 7). Of those, over 1,100 lengths, 400 weights, and 260 otoliths were pollock (Table 9). An additional ~2,800 and 400 pollock lenghts and weights, respectively, were collected from trawls on the cross-shelf transects (Table 9).

Most adult pollock (≥ 34 cm; 70% of males and females) sampled in the core area were in the developing maturity stage (Fig. 4). The mean weight-at-length of pollock found in the core area during the summer of 2022 were within a standard deviation of the weights-at-length of pollock observed during previous summer EBS surveys (Fig. 5).

Acoustic Backscatter

About 49.5% of the total acoustic backscatter observed in the core survey area between 16 m below the surface and 3 m off bottom (the midwater layer) during the 2022 survey was attributed to pollock. This was higher than the fraction of pollock backscatter observed in 2018 (35%), more similar to the fraction of pollock backscatter observed in 2016 (52%), 2014 (45%) and 2012 (56%), and much less than that observed in 2010 (82%; McCarthy et al. 2020; Honkalehto et al. 2018; Honkalehto and McCarthy 2015; Honkalehto et al. 2013, 2012). The western-most transects tend to have fewer and lower density non-pollock backscatter layers compared with transects to the east. Pollock in 2022 were observed in a variety of aggregations including near-bottom layers, small dense schools (cherry balls) in midwater, and diffuse aggregations of individual fish. The remaining non-pollock midwater backscatter in the core area was attributed to an undifferentiated plankton-fishes mixture (33%), or in a few isolated areas, to other fishes (0.05%). In the northern extension area, about 2.5% of the backscatter was attributed to pollock and 21% of the backscatter was attributed to age-0 pollock. The near-bottom analysis (0.5-3.0 m above the seafloor) attributed ~78% of the backscatter in that zone in

the core survey area to pollock, and ~86% of the backscatter in the near-bottom zone of the northern extension area to pollock.

Abundance Estimates

A total of 9.67 billion midwater age-1+ pollock weighing 3.83 million t (Tables 10-14) were estimated in the core survey area on the U.S. Bering Sea shelf in 2022 between 16 m from the surface and within 0.5 m of the bottom. This is just over a 50% increase from the estimate of 5.55 billion fish with a biomass of 2.50 million t in 2018 (McCarthy et al. 2020), the last time a standard acoustic-trawl survey was conducted on the eastern Bering Sea shelf. This is a 6% increase over the estimate of 3.62 million t in 2020 made by the acoustics-only Saildrone survey (De Robertis et al. 2021). The relative estimation error for the pollock biomass estimate to within 0.5 m off bottom was 0.068, which was almost double that of 2018 (0.039, Table 10), and is largely a result of increasing the transect spacing by 100% in most of the core area in 2022. Pollock were observed throughout the surveyed area between the 100- and 200-m isobaths, but the majority of the pollock biomass in the survey was found just north of Unimak Pass and in the northwestern-most portion of the core area where the transects were spaced 20 nmi apart (Fig. 6). Pollock east of 170° W numbered 2.99 billion fish and weighed 1.36 million t (36% of the total biomass found in the core survey area, and 31% of the biomass found shelf-wide, including the northern extension). Pollock abundance west of 170° W was 6.68 billion fish weighing 2.47 million t (64% of total core survey area biomass and 57% of the shelf-wide biomass, including the northern extension).

Pollock biomass increased inside the SCA from 0.23 million t in 2018 to 0.40 million t in 2020, to 0.54 million t in 2022 (Table 10). The pollock biomass within the SCA in 2022 was the same as it was in 2016 (0.54 million t). Estimates for the entire core area and the SCA correlate well ($r^2 = 0.72$) throughout the 1994-2022 time series.

The pollock estimate in the northern extension area was 76.6 million fish weighing 0.54 million t, contributing an additional 14% by number and weight compared with the amount of pollock estimated within the core survey area. In the southeastern part of the northern extension, fish, particularly age-0 pollock, were found in inshore areas where the seafloor is shallower than 50 m. However, throughout the rest of the northern extension, pollock were sparsely but evenly distributed between the 50- and 100-m isobaths (Fig. 6). The relative

estimation error for the northern extension pollock biomass was 0.064, which is comparable to the relative estimation error for the core area, and indicates a similar level of dispersion of pollock biomass between the two areas.

Pollock Length and Age Composition

Pollock lengths were quite consistent throughout the core area, ranging between 30 and 50 cm FL (Tables 11-12); however, as has been seen in the past, the modal length tended to decline to the west. Pollock had a mode of 40 cm FL east of 170° W, whereas they had a mode of 36 cm FL west of 170° W (Fig. 7). Pollock found within the northern extension were mostly larger, ranging between 35 cm and 60 cm FL, with a mode of 50 cm FL; however, there was a smaller mode around 11 cm FL in the northern extension that was absent in the core area (Fig. 7). Pollock length compositions along the cross-shelf transects were similar to those observed during the survey of the core area (Fig. 7), even though the cross-shelf transects were surveyed 3-4 weeks later.

Age-4 pollock (2018 year class) dominated the pollock population in the core survey area (65% of the core area biomass), followed by age-5 pollock (2017 year class, 10% of the core area biomass; Table 14). Age-4 pollock composed 60% of the biomass east of 170° W and 72% of the biomass west of 170° W (Fig. 8a, b). Age-9 pollock (2013 year class) were the dominant aged pollock in the northern extension (25% by biomass), followed closely by age-8 pollock (2014 year class, 24% of the northern extension biomass; Fig. 8c). Very few age-1 and age-2 pollock were observed in the core area (1.5% of the core survey area biomass; Table 14). Although there were appreciable numbers of age-1 pollock in the northern extension (10% by numbers, Fig. 8c), they contributed little (0.2%) to the overall age-1+ pollock biomass in this area (Fig. 8c).

Pollock Length and Weight-at-Age

Mean length- and weight-at-age of pollock were plotted against mean data from combined AT surveys between 2004 and 2018 (Fig. 9). Younger fish (≤ age-5) east of 170° W were longer and heavier than the same aged fish found west of 170° W (Fig. 9). This east-west difference supports the use of two age-length keys to convert abundance-at-length to abundance-at-age (see Methods).

Pollock Vertical Distribution

The vertical distribution of pollock ≥ 30 cm FL in the core survey area exhibited subtle differences between east and west of 170° W (Fig. 10). The estimated MWD depth for pollock in the core region east of 170° W was 95 m, 16 m deeper than that observed in 2018 (79 m). Estimated MWD depth for pollock in the core region west of 170° W was 86 m, 11 m shallower than that observed in 2018 (97 m). In addition to being found deeper in the water column, pollock east of 170° W were also found closer to the seafloor (Fig. 10). More than 82% of pollock in the core area east of 170° W were found within 50 m HAB, whereas only 75% of the pollock west of 170° W were found within 50 m HAB.

Historical Population Trends

Spatial distributions of pollock biomass were evaluated in the EBS from 2007 to 2022, for those years in which when the AT survey was conducted. Earlier spatial patterns of pollock backscatter (1999-2006) when the survey was also conducted in early summer (June-July) are presented in prior publications (e.g., Honkalehto et al. 2008, 2010, 2012, 2013; Honkalehto and McCarthy 2015). Pollock spatial distribution trends in midwater showed that overall biomass was relatively low from 2007 to 2012, and the majority of pollock biomass was concentrated west of 170° W during this period (Fig. 11). In 2014 and 2016, the proportion of pollock biomass increased in the southeast portion of the core area, resulting in a more widely distributed spatial pattern of pollock. After 2016, the proportion of pollock backscatter decreased in the southeast, but not to the low levels observed prior to 2014 (Fig. 11 and Table 10). The highest pollock backscatter observed in 2022 was distributed north of Unimak Pass (~165° W) and west of 170° W along the shelf (Fig. 11).

Temporal patterns in pollock numbers and biomass-at-length and biomass-at-age were examined between 0.5 m off-bottom and near-surface. Between 2014 and 2018, the 2012 year class (age-6 pollock in 2018, the second most abundant cohort in the time series since 1994, Fig. 13) and the 2013 year class (age-5 pollock in 2018), had grown to dominate the midwater abundance (Figs. 12 and 13 and Tables 11-14). By 2022, the presence of these two cohorts had expectedly declined as the fish aged. Their combined contribution was only 4.5% and 2% to the 2022 midwater pollock abundance by biomass and numbers, respectively, as age-10 and age-9 fish.

Age-4 fish replaced them as the most dominant cohort in 2022, contributing 65% and 68% to the midwater pollock biomass and numbers, respectively (Figs. 12 and 13 and Tables 11-14).

The EBS pollock population tends to depend on the success of strong year classes at roughly a 3-5 year frequency (Ianelli et al. 2017). Years with good age-1 recruitment are evident in AT survey results (e.g., 1997, 2007- 2010, and 2014) by the presence of relatively large numbers of 1-2 year-olds (Table 13; Fig. 13). The acoustics-only Saildrone survey did not gather information on age-structure, so the 2018 cohort was not observed as age-2 pollock. However, the dominant presence of the 2018 cohort in 2022 indicates it is the most recent strong year class, which in turn suggests the next strong year class will emerge sometime between 2021 and 2024. There was not a large presence of age-2 (3.4% by numbers) or age-1 (1.5% by numbers) pollock in the core area in 2022 (Fig. 13 and Table 13), which indicates that neither the 2020 nor 2021 cohorts are strong year classes.

Spatial distributions of non-pollock backscatter observed at 38 kHz ("non-pollock backscatter") were also evaluated in the EBS from 2007 to 2022, for those years in which when the AT survey was conducted. Non-pollock backscatter is assumed to represent a temporally-varying mixture of largely unidentified zooplankton and fishes, sometimes including age-0 pollock. This backscatter has varied spatially over the AT survey time series. Most non-pollock backscatter has been observed in the upper part of the water column above the thermocline (Honkalehto et al. 2008). Non-pollock backscatter observed in 2022 consisted of three patches: one on the west side of Bristol Bay, extending northwest into the northern extension; the second on the mid-shelf surrounding the Pribilof Islands; and the third south and west of St. Matthew Island, in the northwest portion of the core area (Fig. 14). Non-pollock backscatter observed in 2004 covered large portions of the survey area on the middle shelf from the Alaska Peninsula to Cape Navarin, Russia (see Honkalehto et al. 2018, Fig. 20). It diminished during years of relatively cold Bering Sea conditions between 2006 and 2010 and has been more widespread in recent years (Fig. 14). Concentrations were observed near the Pribilof Islands in most years since 2007 (2009-2010 being the exception). This backscatter information should be interpreted with caution because the biological composition of the scatterers is unknown.

Cross-Shelf Transect Spatial Autocorrelation

The fitted decorrelation distances (or "range", the distance beyond which samples are no longer spatially correlated) in all three empirical variograms were comparable in magnitude, though the north-south range of 115 km (62 nmi) was longer than the cross-transect range 59 km (32 nmi). The range of the omnidirectional (isotropic) variogram model was longest of all at 136 km (73 nmi; Fig. 15). These results are comparable to those reported for EBS pollock by Walline (2007; 41 to 137 nmi for pollock s_A). They provide some evidence for spatial anisotropy (differences in spatial autocorrelation depending on the direction), suggesting fish distributions were patchier along the cross-transect than along the transects. Furthermore, this suggests that biomass on adjacent transects was only weakly correlated. This was borne out by the Ljung-Box test on the 1D transect averages, which did not show strong evidence of spatial dependence ($p = 0.62$). Based on the fitted variograms and theoretical calculations (Petitgas 1993), it is estimated the 1D relative estimation error given in this report is approximately 1.4 times what it would have been with 20 nmi transect spacing.

The maximum useful transect spacing depends on the requirements of a fishery survey and the spatial structure of the fish population, which may change from year to year. In the extreme case, even a single transect can provide a (low-precision) estimate of abundance, but if a reliable map of the population's distribution is desired, transects must be spaced closer than the fitted decorrelation distances (Simmonds and MacLennan 2005). The 40 nmi transect spacing in 2022 was less than the north-south and isotropic variogram ranges, but greater than the cross-shelf range, suggesting that the transect resolution of the survey was marginal for mapping purposes. Further decreases in survey resolution would risk adjacent transects becoming fully decorrelated, preventing effective mapping and leading to nonlinear increases in estimation variance. Nevertheless, based on our analysis here, and similar results for the reduced-resolution acoustics-only Saildrone survey in 2020 (De Robertis et al. 2021), 40 nmi spacing was acceptable for biomass estimation, albeit with a 40%-100% increase in relative estimation error compared with the usual 20 nmi spacing (Walline 2007, Simmonds and MacLennan 2005).

CITATIONS

Bodholt, H., and H. Solli. 1992. Split beam techniques used in Simrad EK500 to measure target strength. Pages 16–31 *In* World Fisheries Congress. May 1992, Athens, Greece.

De Robertis, A., and K. Williams. 2008. Weight-length relationships in fisheries studies: The standard allometric model should be applied with caution. Trans. Am. Fish. Soc. 137:707–719.

De Robertis, A., D. R. McKelvey, and P. H. Ressler. 2010. Development and application of an empirical multifrequency method for backscatter classification. Can. J. Fish. Aquat. Sci. 67:1459–1474.

De Robertis, A., and K. Taylor. 2014. *In situ* target strength measurements of the scyphomedusa *Chrysaora melanaster*. Fish. Res. 153:18-23.

De Robertis, A., K. Taylor, K. Williams, and C. D. Wilson. 2017a. Species and size selectivity of two midwater trawls used in an acoustic survey of the Alaska Arctic. Deep Sea Res. Part II 135:40–50.

De Robertis, A., K. Taylor, C. D. Wilson, and E. V. Farley. 2017b. Abundance and distribution of Arctic cod (*Boreogadus saida*) and other pelagic fishes over the U.S. Continental Shelf of the Northern Bering and Chukchi Seas. Deep Sea Res. Part II 135:51–65.

De Robertis, A., M. Levine, N. Lauffenburger, T. Honkalehto, J. Ianelli, C. Monnahan, R. Towler, D. Jones, S. Stienessen, and D. McKelvey. 2021. Uncrewed surface vehicle (USV) survey of walleye pollock, *Gadus chalcogrammus*, in response to the cancellation of ship-based surveys. ICES J. Mar. Sci. 78(8): 2797–2808.

Demer, D. A., L. Berger, M. Bernasconi, E. Bethke, K. Boswell, D. Chu, R. Domokos, A. Dunford, S. Fässler, S. Gauthier, L. T. Hufnagle, J. M. Jech, N. Bouffant, A. Lebourges-Dhaussy, X. Lurton, G. J. Macaulay, Y. Perrot, T. Ryan, S. Parker-Stetter, S. Stienessen, T. Weber, and N. Williamson. 2015. Calibration of acoustic instruments. ICES Coop. Res. Rep. 326. 133p.

Foote, K. G. 1987. Fish target strengths for use in echo integrator surveys. J. Acoust. Soc. Am. 82:981–987.

Foote, K. G., H. P. Knudson, G. Vestnes, and E. J. Simmonds. 1987. Calibration of acoustic instruments for fish density estimation: A practical guide. ICES Coop. Res. Rep. 144:69.

Foote, K. G., and J. J. Traynor. 1988. Comparisons of walleye pollock target strength estimates determined from *in situ* measurements and calculations based on swimbladder form. J. Acoust. Soc. Am. 83:9–17.

Gauthier, S., and J. K. Horne. 2004. Acoustic characteristics of forage fish species in the Gulf of Alaska and Bering Sea based on Kirchhoff-approximation models. Can. J. Fish. Aquat. Sci. 61:1839–1850.

Guttormsen, M. A., and C. D. Wilson. 2009. *In situ* measurements of capelin (*Mallotus villosus*) target strength in the North Pacific Ocean. ICES J. Mar. Sci. 66:258–263.

Honkalehto, T., N. Williamson, D. Jones, A. McCarthy, and D. McKelvey. 2008. Results of the echo integration-trawl survey of walleye pollock (*Theragra chalcogramma*) on the U.S. and Russian Bering Sea Shelf in June and July 2007. U.S. Dep. Commer., NOAA Tech. Memo. NMFS-AFSC-190, 53 p.

Honkalehto, T., A. McCarthy, P. Ressler, S. Stienessen, and D. Jones. 2010. Results of the acoustic-trawl survey of walleye pollock (*Theragra chalcogramma*) on the U.S. and Russian Bering Sea shelf in June - August 2009 (DY0909). AFSC Processed Rep. 2010-03, 57 p. Alaska Fish. Sci. Cent., NOAA, Natl. Mar. Fish. Serv., 7600 Sand Point Way NE, Seattle WA 98115.

Honkalehto, T., W. Patton, S. de Blois, and N. Williamson. 2002. Echo integration-trawl survey results for walleye pollock (*Theragra chalcogramma*) on the Bering Sea shelf and slope during summer 2000. U.S. Dep. Commer., NOAA Tech. Memo. NMFS-AFSC-126, 66 p.

Honkalehto, T., A. McCarthy, P. Ressler, K. Williams, and D. Jones. 2012. Results of the acoustic-trawl survey of walleye pollock (*Theragra chalcogramma*) on the U.S. and Russian Bering Sea shelf in June - August 2010 (DY1006). AFSC Processed Rep. 2012-01, 57 p. Alaska Fish. Sci. Cent., NOAA, Natl. Mar. Fish. Serv., 7600 Sand Point Way NE, Seattle WA 98115.

Honkalehto, T., A. McCarthy, P. Ressler, and D. Jones. 2013. Results of the acoustic-trawl survey of walleye pollock (*Theragra chalcogramma*) on the U.S. and Russian Bering Sea shelf in June - August 2012 (DY1207). AFSC Processed Rep. 2013-02, 60 p. Alaska Fish. Sci. Cent., NOAA, Natl. Mar. Fish. Serv., 7600 Sand Point Way NE, Seattle WA 98115.

Honkalehto, T., and A. McCarthy. 2015. Results of the acoustic-trawl survey of walleye pollock (*Theragra chalcogramma*) on the U.S. and Russian Bering Sea shelf in June - August 2014 (DY1407). AFSC Processed Rep. 2013-02, 60 p. Alaska Fish. Sci. Cent., NOAA, Natl. Mar. Fish. Serv., 7600 Sand Point Way NE, Seattle WA 98115.

Honkalehto, T., A. McCarthy, and N. Lauffenburger. 2018. Results of the acoustic-trawl survey of walleye pollock (*Gadus chalcogrammus*) on the U.S. Bering Sea shelf in June - August 2016 (DY1608). AFSC Processed Rep. 2018-03, 78 p. Alaska Fish. Sci. Cent., NOAA, Natl. Mar. Fish. Serv., 7600 Sand Point Way NE, Seattle WA 98115.

Honkalehto, T., A. McCarthy, M. Levine, D. Jones, and K. Williams. 2022. Results of the acoustic-trawl survey of walleye pollock (*Gadus chalcogrammus*) in Shelikof Strait and Marmot Bay March 2021 (DY-202102). AFSC Processed Rep. 2022-08, 78 p. Alaska Fish. Sci. Cent., NOAA, Natl. Mar. Fish. Serv., 7600 Sand Point Way NE, Seattle WA 98115.

Ianelli, J. N., S. Kotwicki, T. Honkalehto, K. Holsman, and B. Fissel, 2017. Assessment of the walleye pollock stock in the eastern Bering Sea, p. 55-184. *In* Stock assessment and fishery evaluation report for the groundfish resources of the Bering Sea/Aleutian Islands regions. North Pacific Fishery Management Council, 605 W. 4th Ave., Anchorage, AK 99501-2252.

Jech, J. M., K. G. Foote, D. Chu, and L. C. Hufnagle. 2005. Comparing two 38-kHz scientific echosounders. ICES J. Mar. Sci. 62:1168–1179.

Jones, D. T., A. De Robertis, and N. J. Williamson. 2011. Statistical combination of multi-frequency sounder-detected bottom lines reduces bottom integrations. U.S. Dep. Commer., NOAA Tech Memo. NMFS-AFSC-219, 13 p.

Jones, D. T., N. E. Lauffenburger, K. Williams, and A. De Robertis. 2019. Results of the acoustic-trawl survey of walleye pollock (*Gadus chalcogrammus*) in the Gulf of Alaska, June-August 2017 (DY2017-06). AFSC Processed Rep. 2019-08, 110 p. Alaska Fish. Sci. Cent., NOAA, Natl. Mar. Fish. Serv., 7600 Sand Point Way NE, Seattle WA 98115.

Jones, D. T., M. Levine, K. Williams, and A. De Robertis. 2022. Results of the acoustic-trawl survey of walleye pollock (*Gadus chalcogrammus*) in the Gulf of Alaska, May-August 2019 (DY2019-06). AFSC Processed Rep. 2022-07, 118 p. Alaska Fish. Sci. Cent., NOAA, Natl. Mar. Fish. Serv., 7600 Sand Point Way NE, Seattle WA 98115.

Kang, D., T. Mukai, K. Iida, D. Hwang, and J.-G. Myoung. 2005. The influence of tilt angle on the acoustic target strength of the Japanese common squid (*Todarodes pacificus*). ICES J. Mar. Sci. 62:779–789.

Lauffenburger, N., A. De Robertis, S. Kotwicki. 2017. Combining bottom trawls and acoustics in a diverse semipelagic environment: What is the contribution of walleye-pollock (*Gadus chalcogrammus*) to near-bottom acoustic backscatter in the eastern Bering Sea?. Can. J. Fish. Aquat. Sci. 74:256-264.

Ljung and Box. 1978. On a measure of lack of fit in time series models. Biometrika 65 (2), 297–303. https://doi.org/10.1093/biomet/65.2.297.

Levine, M., D. Jones, and D. McGowan. 2024. Results of the acoustic-trawl survey of walleye pollock (*Gadus chalcogrammus*) in the Gulf of Alaska, June-July 2021 (DY2021-04). AFSC Processed Rep. 2024-07, 100 p. Alaska Fish. Sci. Cent., NOAA, Natl. Mar. Fish. Serv., 7600 Sand Point Way NE, Seattle WA 98115. https://repository.library.noaa.gov/view/noaa/61451

Markowitz, E. H., Dawson, E. J., Anderson, C. B., Rohan, S. K., Charriere, N. E., Prohaska, B. K., and Stevenson, D. E. 2023. Results of the 2022 eastern and northern Bering Sea continental shelf bottom trawl survey of groundfish and invertebrate fauna. U.S. Dep. Commer., NOAA Tech. Memo. NMFS-AFSC-469, 213 p.

MacLennan, D. N., P. G. Fernandes, and J. Dalen. 2002. A consistent approach to definitions and symbols in fisheries acoustics. ICES J. Mar. Sci. 59:365–369.

McCarthy, A., T. Honkalehto, N. Lauffenburger, and A. De Robertis. 2020. Results of the acoustic-trawl survey of walleye pollock (*Gadus chalcogrammus*) on the U. S. Bering Sea shelf in June – August 2018 (DY1807). AFSC Processed Rep. 2020-07, 83 p. Alaska Fish. Sci. Cent., NOAA, Natl. Mar. Fish. Serv., 7600 Sand Point Way NE, Seattle, WA 98115.

Methot, R. D. 1986. Frame trawl for sampling pelagic juvenile fish. CalCOFI Rep. Vol. XXVII: 267-278.

Miller, D. M. 1984. Reducing transformation bias in curve fitting. Am. Stat. 38:124–126.

Ona, E. 2003. An expanded target-strength relationship for herring. ICES J. Mar. Sci. 60:493–499.

Ona, E., and R. B. Mitson. 1996. Acoustic sampling and signal processing near the seabed: The deadzone revisited. ICES J. Mar. Sci. 53:677–690.

Overland, J.E., S.A. Salo, L.H. Kantha, and C.A. Clayson. 1999. Thermal stratification and mixing on the Bering Sea shelf, p. 129-146. *In* T.R. Loughlin and K. Ohtani (eds.), Dynamics of the Bering Sea: a summary of physical, chemical and biological characteristics and a synopsis of research on the Bering Sea. Sydney, British Columbia and Fairbanks, Alaska: North Pacific Marine Science Organization (PICES), and University of Alaska Sea Grant College Program AK-SG-99-03.

Petitgas, P. 1993. Geostatistics for fish stock assessments: A review and an acoustic application. ICES J. Mar. Sci. 50:285–298.

Ressler, P. 2022. Eastern Bering Sea Euphausiids ('Krill'), pp. 91-93. *In* Siddon, E. (ed.), Ecosystem Status Report 2022: Eastern Bering Sea, Stock Assessment and Fishery Evaluation Report, North Pacific Fishery Management Council, 1007 West 3rd Ave., Suite 400, Anchorage, Alaska 99501. URL: https://apps-afsc.fisheries.noaa.gov/REFM/docs/2022/EBSecosys.pdf.

Rivoirard, J., J. Simmonds, K. G. Foote, P. Fernandes, and N. Bez. 2000. Geostatistics for estimating fish abundance. Blackwell Science Ltd, Oxford, UK. 216 p.

Simmonds, E. J., and D. N. MacLennan. 2005. Fisheries acoustics: Theory and practice. 2nd edition. Blackwell Science Ltd, Oxford, UK. 472 p.

Simrad. 2018. Reference manual for simrad EK80 scientific echo sounder application. Strandpromenenaden 50, Box 111, N-3191 Horten, Norway.

Towler, R., and K. Williams. 2010. An inexpensive millimeter-accuracy electronic length measuring board. Fish. Res. 106:107–111.

Traynor, J. J. 1996. Target-strength measurements of walleye pollock (*Theragra chalcogramma*) and Pacific whiting (*Merluccius productus*). ICES J. Mar. Sci. 53:253–258.

Walline, P. D. 2007. Geostatistical simulations of eastern bering sea walleye pollock spatial distributions, to estimate sampling precision. ICES J. Mar. Sci. 64:559–569.

Williams, K., A. E. Punt, C. D. Wilson, and J. K. Horne. 2011. Length-selective retention of walleye pollock, *Theragra chalcogramma*, by midwater trawls. ICES J. Mar. Sci. 68:119–129.

Williams, K., C. N. Rooper, and R. Towler. 2010. Use of stereo camera systems for assessment of rockfish abundance in untrawlable areas and for recording pollock behavior during midwater trawls. Fish. Bull., U.S. 108:352–362.

Williams, K., R. Towler, P. Goddard, R. Wilborn, and C. Rooper. 2016. SEBASTES Stereo Image Analysis Software. AFSC Processed Rep. 2016-03, 42 p. Alaska Fish. Sci. Cent., NOAA, Natl. Mar. Fish. Serv., 7600 Sand Point Way NE, Seattle WA 98115.

Williamson, N. J., and J. J. Traynor. 1996. Application of a one-dimensional geostatistical procedure to fisheries acoustic surveys of Alaskan pollock. ICES J. Mar. Sci. 53:423–428.

Wyllie-Echeverria T., and W. Wooster. 1998. Year-to-year variations in Bering Sea ice cover and some consequences for fish distributions. Fish. Oceanogr. 7: 159−170.

Table 1. -- Simrad EK80 38 kHz acoustic system description and settings used during the summer 2022 Eastern Bering Sea acoustic-trawl survey. These include environmental parameters and results from standard sphere acoustic system calibrations conducted in association with the survey and final values used to calculate biomass & abundance data. The collection settings column contains 1 June EK80 calibration utility results. Other columns are a combination of on-axis and EK80 calibration utility results (see Methods and Results and Discussion sections of text for details).

		Survey collection settings	31 May Captain's Bay Unalaska	9 July Captain's Bay Unalaska	5 Aug Captain's Bay Unalaska	Final analysis settings
Echosounder		Simrad EK80	--	--	--	Simrad EK80
Transducer		ES38-7 s/n 324	--	--	--	ES38-7 s/n 324
Frequency (kHz)		38	--	--	--	38
Transducer depth (m)		9.15	--	--	--	9.15
Pulse length (ms)		0.512	--	--	--	0.512
Transmitted power (W)		2000	--	--	--	2000
Angle sensitivity	Along	18.00	--	--	--	18.00
	Athwart	18.00	--	--	--	18.00
2-way beam angle (dB)		-20.70	--	--	--	-20.50
Gain (dB)		27.19	27.13	27.06	27.23	27.14
s_A correction (dB)		-0.10	-0.09	-0.11	-0.10	-0.10
Integration gain (dB)		27.09	27.04	26.95	27.12	27.04
3 dB beamwidth	Along	6.59	6.59	6.68	6.72	6.66
	Athwart	6.70	6.70	6.67	6.57	6.65
Angle offset	Along	-0.03	-0.03	-0.04	-0.06	-0.04
	Athwart	0.08	0.08	0.07	0.12	0.09
Post-processing sv threshold (dB)		-70	--	--	--	--
Measured standard sphere TS (dB)		--	-42.30	-42.41	-42.11	--
Sphere range from transducer (m)		--	20.47	21.15	19.39	--
Absorption coefficient (dB/m)		0.009978	0.009951	0.009838	0.009783	0.009978
Sound velocity (m/s)		1470.0	1465.1	1472.0	1475.4	1470.0
Water temp at transducer (°C)		--	4.9	7.2	8.3	--

Note: Gain and beam pattern terms are defined in Demer et al., 2015.

Table 2. -- Target strength (TS) to size relationships from the literature used to allocate 38 kHz acoustic backscatter to most species in this report. The symbols in the equations are as follows: r is the bell radius in centimeters and L is length in centimeters for all groups except pelagic crustaceans, in which case L is in meters.

Group	TS (dB re 1 m^2)	Length type	TS derived for which species	Reference
Walleye pollock	$TS = 20 \log_{10} L\text{-}66$	L = fork length	*Gadus chalcogrammus*	Foote and Traynor (1988), Traynor (1996)
Pacific capelin	$TS = 20 \log_{10} L\text{-}70.3$	L = total length	*Mallotus catervarius*	Guttormsen and Wilson (2009)
Pacific herring	$TS = 20 \log_{10} L\text{-}2.3 \log_{10}(1 + depth/10) - 65.4$	L = fork length	*Clupea harengus*	Ona (2003)
Eulachon	$TS = 20 \log_{10} L - 84.5$	L = total length	*Thaleichthys pacificus*	Gauthier and Horne (2004)
Fish with swim bladders	$TS = 20 \log_{10} L - 67.4$	L = total length	Physoclist fishes	Foote et al. (1987)
Fish without swim bladders	$TS = 20 \log_{10} L - 83.2$	L = total length	*Pleurogrammus monopterygius*	Gauthier and Horne (2004)
Jellyfish	$TS = 10 \log_{10}(\pi r^2) - 86.8$	r = bell radius	*Chrysaora melanaster*	De Robertis and Taylor (2014)
Squid	$TS = 20 \log_{10} L - 75.4$	L = mantle length	*Todarodes pacificus*	Kang et al. (2005)
Pelagic crustaceans[1]	$TS = A * (\log_{10}(BkL)/(BkL))^c + D((kL)^6) + E((kL)^5) + F((kL)^4) + G((kL)^3) + H((kL)^2) + I(kL) + J + 20 \log_{10}(L/L_0)$	L = total length	*Euphausia superba*	Demer and Conti (2005)

[1]A = -930.429983; B = 3.21027896; C = 1.74003785; D = 1.36133896 x 10^{-8}; E = -2.26958555 x 10^{-6}
F= 1.50291244 x 10^{-4}; G = -4.86306872 x 10^{-3}; H = 0.0738748423; I = -0.408004891; J = -73.9078690; and L_0 = 0.03835
If L < 0.015 m, TS = -105 dB; and if L > 0.065 m, TS = -73 dB.
k = 2πfc, where f = 38,000 (frequency in Hz) and c = 1470 (sound speed in m/s).

Table 3. -- Trawl stations and catch data summary from the summer 2022 EBS acoustic-trawl survey in the East of 170, SCA, West of 170, EBS Northern Extension, and EBS Cross Transect regions.

Haul	Area	Gear	Date	Time	Duration	Start Position		Depth (m)		Temp (°C)		walleye pollock		Other
No.		Type[a]	(GMT)	(GMT)	(mins)	Lat. (N)	Long. (W)	Headrope[b]	Bottom	Headrope	Surface[c]	(kg)	Number	(kg)
1	East of 170	Methot	4-Jun	04:11	0.4	56.5442	-162.7747	43	78	3.0	10.3	-	-	2.4
2	SCA	LFS1421	5-Jun	00:36	15.1	55.4779	-163.9810	67	92	3.1	8.2	566.6	1,249	326.4
3	SCA	83/112	5-Jun	03:55	29.6	55.4613	-163.9885	80	93	3.1	8.2	4.7	11	136.0
4	East of 170	LFS1421	6-Jun	17:45	36.6	56.1579	-165.1919	65	94	2.5	8.1	1,822.1	4,338	127.9
5	SCA	LFS1421	7-Jun	02:32	5.4	55.0011	-165.1394	84	111	4.5	6.7	765.6	1,831	18.9
6	SCA	LFS1421	7-Jun	17:37	6.4	54.6336	-165.1541	64	84	4.4	5.6	1,180.1	2,185	455.7
7	East of 170	LFS1421	8-Jun	22:52	2.4	56.2311	-166.3844	76	110	3.3	8.7	1,239.0	3,088	25.9
8	East of 170	LFS1421	9-Jun	02:59	48.7	56.6192	-166.4071	61	86	2.3	9.2	1,583.2	3,455	64.0
9	East of 170	LFS1421	10-Jun	03:47	25.1	57.1696	-167.6883	51	76	1.6	7.3	748.2	997	95.8
10	East of 170	LFS1421	10-Jun	17:34	21.0	56.7615	-167.6521	67	94	2.3	7.5	2,373.0	5,195	577.0
11	East of 170	LFS1421	11-Jun	00:23	18.8	56.0934	-167.5917	104	137	4.1	8.2	933.9	2,170	0.4
12	East of 170	LFS1421	11-Jun	17:36	31.5	55.7364	-168.7304	129	157	4.0	7.5	725.1	1,392	2,529.9
13	East of 170	LFS1421	12-Jun	03:49	18.4	56.3188	-168.8249	72	126	3.4	7.7	454.8	1,071	1.5
14	East of 170	LFS1421	12-Jun	17:26	6.0	56.8867	-168.8971	64	84	3.0	6.6	3,649.9	8,228	13.1
15	West of 170	LFS1421	15-Jun	00:26	4.0	57.4121	-170.2047	40	63	1.7	5.5	441.3	652	87.7
16	West of 170	LFS1421	23-Jun	00:55	23.4	56.7022	-171.3191	92	119	3.7	7.6	1,400.0	3,028	0.4
17	West of 170	LFS1421	23-Jun	17:34	25.2	57.7782	-171.5159	77	99	1.5	6.4	778.1	1,886	81.1
18	West of 170	Methot	24-Jun	03:09	30.1	59.1575	-171.7719	56	84	-	5.6	-	-	3.7
19	West of 170	LFS1421	25-Jun	19:09	15.3	59.0647	-173.0641	63	106	1.0	6.6	549.3	1,510	103.1
20	West of 170	Methot	26-Jun	00:10	30.0	58.5886	-172.9649	42	112	3.1	6.9	-	-	22.0
21	West of 170	LFS1421	26-Jun	02:33	31.4	58.5547	-172.9420	87	112	2.4	7.1	718.9	2,818	31.9
22	West of 170	LFS1421	26-Jun	17:40	13.9	57.6700	-172.7523	92	119	3.3	7.2	1,527.4	3,003	2.2
23	West of 170	LFS1421	26-Jun	22:46	52.5	57.4183	-172.6928	79	118	4.0	7.3	91.6	163	5.2
24	West of 170	83/112	27-Jun	02:46	20.1	57.2406	-172.6554	111	115	3.0	7.4	1,124.3	1,665	97.5
25	West of 170	LFS1421	27-Jun	20:31	44.6	57.5154	-173.9638	-	183	-	7.0	215.1	237	5.3
26	West of 170	LFS1421	28-Jun	03:40	19.1	58.3744	-174.1822	114	138	3.7	7.5	4.8	11	12.3
27	West of 170	LFS1421	28-Jun	18:39	18.7	58.7858	-174.3083	104	138	3.1	7.2	968.5	2,868	3.5
28	West of 170	LFS1421	29-Jun	00:10	17.4	59.3305	-174.4486	63	121	2.3	7.5	1,528.2	5,176	98.2
29	West of 170	LFS1421	29-Jun	18:22	28.5	60.2719	-174.6960	78	105	0.9	6.2	833.8	2,214	50.2
30	West of 170	LFS1421	29-Jun	23:56	40.7	60.8773	-174.8577	62	95	0.1	6.5	1,219.2	3,695	71.9
31	West of 170	LFS1421	30-Jun	17:56	14.4	61.3678	-176.3900	76	109	0.2	7.4	1,318.5	4,293	43.2
32	West of 170	LFS1421	1-Jul	02:43	30.1	60.5621	-176.1400	96	121	1.3	7.1	721.5	2,432	59.4
33	West of 170	LFS1421	1-Jul	21:02	20.8	59.2926	-175.7293	104	138	2.0	7.6	715.2	2,172	23.0

Haul	Area	Gear	Date	Time	Duration	Start Position		Depth (m)		Temp (°C)		walleye pollock		Other
No.		Type[a]	(GMT)	(GMT)	(mins)	Lat. (N)	Long. (W)	Headrope[b]	Bottom	Headrope	Surface[c]	(kg)	Number	(kg)
34	West of 170	LFS1421	2-Jul	01:53	28.5	59.0270	-175.6512	60	134	3.4	7.8	1,862.8	5,549	18.5
35	West of 170	LFS1421	2-Jul	17:24	58.3	58.6499	-176.8190	129	164	3.6	7.6	344.7	866	6.2
36	West of 170	LFS1421	3-Jul	00:17	21.5	59.1337	-176.9803	124	147	3.0	7.9	950.9	2,906	19.8
37	West of 170	LFS1421	3-Jul	17:30	16.8	60.1341	-177.3353	88	139	1.7	8.2	677.5	2,397	14.1
38	West of 170	LFS1421	3-Jul	20:36	33.5	60.1936	-177.3607	67	139	1.8	8.1	330.5	1,119	20.7
39	West of 170	LFS1421	4-Jul	02:22	39.1	60.6699	-177.5399	111	149	1.5	8.2	746.1	3,353	9.7
40	West of 170	LFS1421	4-Jul	17:37	25.5	60.6218	-178.8733	193	251	2.8	8.4	369.6	1,298	34.5
41	West of 170	LFS1421	4-Jul	22:46	4.8	60.2624	-178.6886	174	375	3.4	8.3	2,721.3	6,825	24.7
42	West of 170	LFS1421	5-Jul	03:16	1.5	59.9126	-178.5819	101	142	1.7	8.5	913.6	2,840	34.0
43	West of 170	LFS1421	5-Jul	17:49	36.2	58.7526	-177.4715	127	161	3.6	7.6	360.5	840	8.9
44	West of 170	LFS1421	6-Jul	02:14	7.9	59.7513	-177.8381	97	152	2.6	8.3	537.5	1,493	15.4
45	West of 170	LFS1421	6-Jul	17:37	4.1	60.0758	-177.9629	104	145	1.5	8.5	769.3	2,363	20.8
46	West of 170	LFS1421	6-Jul	20:55	3.8	60.4166	-178.0936	125	158	1.8	8.8	1,313.8	5,199	21.3
47	West of 170	LFS1421	7-Jul	01:54	18.3	60.9384	-178.2929	132	161	1.8	9.1	391.8	1,342	15.0
48	West of 170	LFS1421	7-Jul	18:34	14.2	61.1617	-177.6281	114	140	1.4	8.7	667.1	2,467	14.6
49	EBS Northern Extension	LFS1421	21-Jul	17:59	20.1	57.2626	-161.5008	14	58	8.2	8.6	0.9	5	155.8
50	EBS Northern Extension	LFS1421	22-Jul	00:03	20.4	57.9894	-161.3982	27	54	5.5	8.7	13.4	15	61.8
51	EBS Northern Extension	LFS1421	22-Jul	03:31	20.1	58.2201	-161.3788	20	44	8.0	8.8	1.0	1	48.5
52	EBS Northern Extension	83/112	22-Jul	18:16	15.3	58.0549	-162.6742	35	39	8.0	8.6	4.1	3	18.7
53	EBS Northern Extension	LFS1421	22-Jul	22:11	20.3	57.6184	-162.7003	18	46	6.7	8.7	1.8	2	34.2
54	EBS Northern Extension	LFS1421	23-Jul	02:51	15.3	57.2394	-162.7251	31	55	5.2	9.2	8.9	39	103.9
55	EBS Northern Extension	LFS1421	23-Jul	17:31	20.4	57.5985	-163.9388	29	51	4.2	8.4	8.8	91	43.4
56	EBS Northern Extension	LFS1421	24-Jul	03:19	20.2	58.2777	-165.1335	24	46	6.3	7.0	4.2	9	57.8
57	EBS Northern Extension	LFS1421	24-Jul	17:44	16.5	57.3596	-165.2068	16	67	9.0	9.2	1.8	2	40.2
58	EBS Northern Extension	LFS1421	25-Jul	01:04	42.5	58.0529	-166.4826	34	59	1.6	7.4	41.9	51	8.9
59	EBS Northern Extension	LFS1421	25-Jul	18:11	15.3	58.3544	-167.7986	19	59	6.3	6.3	6.7	9	34.2
60	EBS Northern Extension	LFS1421	26-Jul	03:34	46.1	58.7723	-169.1074	40	62	2.1	6.4	66.5	85	11.3
61	EBS Northern Extension	LFS1421	26-Jul	20:10	21.1	59.9011	-169.3113	19	47	6.5	6.6	3.6	5	23.6
62	EBS Northern Extension	LFS1421	28-Jul	03:37	34.4	62.8358	-172.2403	34	56	-1.3	7.1	185.5	254	29.1
63	EBS Northern Extension	LFS1421	28-Jul	23:15	30.2	60.5279	-172.0068	40	63	0.1	7.5	117.0	180	34.0
64	EBS Northern Extension	Methot	29-Jul	20:50	45.3	62.5069	-173.8658	59	67	-	8.5	-	-	6.4
65	EBS Northern Extension	LFS1421	30-Jul	03:38	41.2	62.9651	-174.0187	46	75	-1.4	7.5	30.0	46	31.8
66	EBS Northern Extension	LFS1421	30-Jul	21:08	16.0	61.6623	-175.0166	64	85	-1.4	8.4	249.8	505	72.8
67	EBS Cross Transect	LFS1421	31-Jul	02:54	20.2	61.0671	-175.7236	80	104	0.8	8.6	319.0	760	114.3
68	EBS Cross Transect	LFS1421	31-Jul	17:53	10.4	60.5412	-177.2129	120	147	1.7	10.0	853.8	3,561	17.4

Haul	Area	Gear	Date	Time	Duration	Start Position		Depth (m)		Temp (°C)		walleye pollock		Other
No.		Type[a]	(GMT)	(GMT)	(mins)	Lat. (N)	Long. (W)	Headrope[b]	Bottom	Headrope	Surface[c]	(kg)	Number	(kg)
69	EBS Cross Transect	LFS1421	31-Jul	22:17	3.2	60.2235	-176.9878	104	145	1.9	10.0	935.5	3,626	40.9
70	EBS Cross Transect	LFS1421	1-Aug	03:05	3.1	59.8332	-176.2950	100	140	1.9	9.7	536.2	1,915	6.9
71	EBS Cross Transect	LFS1421	1-Aug	18:14	17.0	59.0381	-174.7890	88	129	3.0	9.8	404.2	1,084	22.3
72	EBS Cross Transect	LFS1421	2-Aug	03:09	13.3	58.1492	-173.1811	74	110	2.9	9.7	461.8	1,198	19.3
73	EBS Cross Transect	LFS1421	2-Aug	18:28	48.9	57.5561	-172.1431	80	110	2.7	9.7	913.1	2,173	5.9
74	EBS Cross Transect	Methot	3-Aug	00:10	30.3	57.3093	-171.7085	87	106	-	9.6	-	-	9.1
75	EBS Cross Transect	LFS1421	3-Aug	03:41	9.4	57.0884	-171.3224	78	106	3.3	9.1	19.8	32	393.8

[a]Methot = Methot plankton net, LFS1421 = LFS1421 midwater trawl, 83/112 = Bering Sea bottom trawl

[b]Headrope depth obtained from SBE temperature logger.

[c]Average temperature measured from an SBE temperature logger

Table 4. -- Catch by species and numbers of length and weight measurements taken from 43 LFS1421 hauls during the 2022 acoustic trawl survey of the Eastern Bering Sea.

		Catch				Measurements	
Species name	Scientific name	Weight (kg)	%	Number	%	Length	Weight
walleye pollock	*Gadus chalcogrammus*	42,029.9	89.0	112,214	93.8	15,364	2,408
Pacific ocean perch	*Sebastes alutus*	2,530.3	5.4	2,862	2.4	88	28
northern sea nettle	*Chrysaora melanaster*	2,441.8	5.2	3,792	3.2	860	386
Pacific herring	*Clupea pallasii*	90.8	0.2	425	0.4	184	82
smooth lumpsucker	*Aptocyclus ventricosus*	44.9	<0.1	44	<0.1	38	38
Aequorea sp.	*Aequorea* sp.	41.7	<0.1	143	0.1	14	14
chum salmon	*Oncorhynchus keta*	19.8	<0.1	13	<0.1	13	13
jellyfish unid.	Scyphozoa (class)	6.0	<0.1	1	<0.1	1	0
northern rock sole	*Lepidopsetta polyxystra*	4.1	<0.1	8	<0.1	8	8
Phacellophora sp.	*Phacellophora* sp.	2.2	<0.1	19	<0.1	16	16
great sculpin	*Myoxocephalus polyacanthocephalus*	1.8	<0.1	1	<0.1	1	1
northern rockfish	*Sebastes polyspinis*	1.8	<0.1	2	<0.1	1	1
pink salmon	*Oncorhynchus gorbuscha*	1.7	<0.1	2	<0.1	2	2
egg yolk jelly	*Phacellophora camtschatica*	1.3	<0.1	7	<0.1	7	6
Aurelia labiata	*Aurelia labiata*	1.1	<0.1	5	<0.1	5	5
Pacific cod	*Gadus macrocephalus*	1.0	<0.1	1	<0.1	1	1
Aurelia sp.	*Aurelia* sp.	0.6	<0.1	5	<0.1	5	5
flathead sole	*Hippoglossoides elassodon*	0.6	<0.1	2	<0.1	2	2
yellowfin sole	*Limanda aspera*	0.5	<0.1	1	<0.1	1	1
Berry armhook squid	*Gonatus berryi*	0.4	<0.1	1	<0.1	1	1
eulachon	*Thaleichthys pacificus*	0.2	<0.1	3	<0.1	1	1
euphausiid unid.	Euphausiacea (order)	0.2	<0.1	0	<0.1	0	0
rock sole unid.	*Lepidopsetta* (genus)	0.1	<0.1	1	<0.1	1	1
Ptychogena sp.	*Ptychogena* (genus)	<0.1	<0.1	5	<0.1	5	0
bivalve unid.	Bivalvia (class)	<0.1	<0.1	1	<0.1	0	0
lions mane	*Cyanea capillata*	<0.1	<0.1	1	<0.1	1	1
sand lance unid.	*Ammodytes* (genus)	<0.1	<0.1	3	<0.1	3	3
isopod unid.	Isopoda (order)	<0.1	<0.1	11	<0.1	0	0
walleye pollock Age 0	*Gadus chalcogrammus*	<0.1	<0.1	83	<0.1	46	0
fish larvae unid.	Actinopterygii (class)	<0.1	<0.1	5	<0.1	5	1
squid unid.	Cephalopoda (class)	<0.1	<0.1	3	<0.1	3	0
salp unid.	Thaliacea (class)	<0.1	<0.1	1	<0.1	0	0
amphipod unid.	Amphipoda (order)	<0.1	<0.1	1	<0.1	0	0
smelt unid.	Osmeridae (family)	<0.1	<0.1	1	<0.1	1	0
Total		47,223.3		119,667		16,678	3,025

Table 5. -- Catch by species and numbers of length and weight measurements taken from 2 83/112 hauls during the 2022 acoustic trawl survey of the Eastern Bering Sea.

		Catch				Measurements	
Species name	Scientific name	Weight (kg)	%	Number	%	Length	Weight
walleye pollock	*Gadus chalcogrammus*	1,128.9	82.9	1,676	89.3	468	72
northern sea nettle	*Chrysaora melanaster*	134.1	9.8	71	3.8	36	11
basketstar	*Gorgonocephalus eucnemis*	33.3	2.4	0	<0.1	0	0
flathead sole	*Hippoglossoides elassodon*	32.9	2.4	99	5.3	35	10
empty gastropod shells	Gastropoda (class)	7.9	0.6	0	<0.1	0	0
Pacific cod	*Gadus macrocephalus*	7.2	0.5	3	0.2	3	3
arrowtooth flounder	*Atheresthes stomias*	6.4	0.5	11	0.6	11	10
sea pen or sea whip unid.	Pennatulacea (order)	3.4	0.3	0	<0.1	0	0
rex sole	*Glyptocephalus zachirus*	1.9	0.1	5	0.3	5	5
giant octopus	*Enteroctopus dofleini*	1.6	0.1	1	<0.1	0	0
Aequorea sp.	Aequorea *sp.*	1.5	0.1	7	0.4	7	7
sea urchin unid.	Echinoidea (class)	1.1	<0.1	0	<0.1	0	0
yellow Irish lord	*Hemilepidotus jordani*	1.0	<0.1	1	<0.1	1	1
jellyfish unid.	Scyphozoa (class)	0.5	<0.1	0	<0.1	0	0
Aurelia labiata	*Aurelia labiata*	0.4	<0.1	1	<0.1	1	1
egg yolk jelly	*Phacellophora camtschatica*	0.2	<0.1	1	<0.1	1	1
Invert. unident. 1	*Invert. unident. 1*	<0.1	<0.1	0	<0.1	0	0
Total		1,362.5		1,876		568	121

Table 6. -- Catch by species and numbers of length and weight measurements taken from 16 LFS1421 hauls during the 2022 acoustic trawl survey of the Eastern Bering Sea.

		Catch				Measurements	
Species name	Scientific name	Weight (kg)	%	Number	%	Length	Weight
walleye pollock	*Gadus chalcogrammus*	741.8	48.4	1,299	0.1	1,113	405
northern sea nettle	*Chrysaora melanaster*	389.3	25.4	1,161	0.1	449	168
walleye pollock Age 0	*Gadus chalcogrammus*	348.5	22.7	974,543	99.7	262	0
yellowfin sole	*Limanda aspera*	50.1	3.3	126	<0.1	117	80
jellyfish unid.	Scyphozoa (class)	1.1	<0.1	28	<0.1	1	1
Staurophora mertensi	*Staurophora mertensi*	0.5	<0.1	36	<0.1	13	0
smooth lumpsucker	*Aptocyclus ventricosus*	0.4	<0.1	1	<0.1	1	1
Hydromedusa (unid.)	Hydromedusa (unid.)	0.3	<0.1	75	<0.1	8	7
Pacific cod	*Gadus macrocephalus*	0.3	<0.1	188	<0.1	35	1
Aequorea sp.	*Aequorea* sp.	0.2	<0.1	5	<0.1	1	1
sand lance unid.	*Ammodytes* (genus)	0.2	<0.1	310	<0.1	12	0
rock sole unid.	*Lepidopsetta* (genus)	0.1	<0.1	1	<0.1	1	1
Pacific capelin	*Mallotus catervarius*	<0.1	<0.1	28	<0.1	3	2
fish larvae unid.	Actinopterygii (class)	<0.1	<0.1	41	<0.1	5	0
Pacific sand lance	*Ammodytes personatus*	<0.1	<0.1	74	<0.1	2	0
sea whip unid.	Virgulariidae (family)	<0.1	<0.1	1	<0.1	0	0
amphipod unid.	Amphipoda (order)	<0.1	<0.1	1	<0.1	0	0
Total		1,533.1		977,918		2,023	667

Table 7. -- Catch by species and numbers of length and weight measurements taken from 1 83/112 hauls during the 2022 acoustic trawl survey of the Eastern Bering Sea.

		Catch				Measurements	
Species name	Scientific name	Weight (kg)	%	Number	%	Length	Weight
yellowfin sole	*Limanda aspera*	9.9	43.4	34	2.1	34	10
walleye pollock	*Gadus chalcogrammus*	4.1	18.1	3	0.2	3	3
rock sole unid.	*Lepidopsetta* (genus)	2.3	10.1	32	2.0	32	10
starry flounder	*Platichthys stellatus*	2.1	9.0	1	<0.1	1	1
Asterias sp.	Asterias *sp.*	1.4	6.3	14	0.9	0	0
flathead sole	*Hippoglossoides elassodon*	1.3	5.7	2	0.1	2	2
walleye pollock Age 0	*Gadus chalcogrammus*	0.8	3.6	1,482	93.1	40	0
Pacific herring	*Clupea pallasii*	0.4	1.6	3	0.2	3	3
hermit crab unid.	Paguridae (family)	0.2	1.0	1	<0.1	0	0
northern sea nettle	*Chrysaora melanaster*	0.2	0.9	1	<0.1	1	1
lions mane	*Cyanea capillata*	<0.1	0.3	1	<0.1	1	1
Pacific capelin	*Mallotus catervarius*	<0.1	0.1	5	0.3	5	5
Crangon sp.	*Crangon* sp.	<0.1	<0.1	13	0.8	13	0
Total		22.8		1,592		135	36

Table 8. -- Catch by species and numbers of length and weight measurements taken from 5 Methot hauls during the 2022 acoustic trawl survey of the Eastern Bering Sea.

		Catch				Measurements	
Species name	Scientific name	Weight (kg)	%	Number	%	Length	Weight
northern sea nettle	*Chrysaora melanaster*	39.1	89.8	156	0.3	121	96
euphausiid unid.	Euphausiacea (order)	2.5	5.8	55,300	96.7	0	0
Aurelia labiata	*Aurelia labiata*	0.9	2.0	11	<0.1	11	11
Aequorea sp.	*Aequorea* sp.	0.5	1.1	7	<0.1	7	7
Hydromedusa (unid.)	Hydromedusa (unid.)	0.3	0.6	116	0.2	51	26
jellyfish unid.	Scyphozoa (class)	0.1	0.3	1,269	2.2	0	0
copepod unid.	Maxillopoda (class)	<0.1	0.2	141	0.2	0	0
Ptychogena sp.	*Ptychogena* (genus)	<0.1	<0.1	4	<0.1	4	0
walleye pollock Age 0	*Gadus chalcogrammus*	<0.1	<0.1	112	0.2	28	0
Themisto libellula	*Themisto libellula*	<0.1	<0.1	11	<0.1	0	0
amphipod unid.	Amphipoda (order)	<0.1	<0.1	20	<0.1	0	0
fish larvae unid.	Actinopterygii (class)	<0.1	<0.1	66	0.1	4	0
shrimp unid.	Malacostraca (class)	<0.1	<0.1	1	<0.1	0	0
Total		43.6		57,214		226	140

Table 9. --Numbers of specimens measured and biological samples collected during the 2022 EBS acoustic-trawl survey.

Haul	Region	Pollock age 1+					Pollock age 0		Other	
No.	Name	Lengths	Weights	Maturities	Otoliths	Ovaries	Lengths	Weights	Lengths	Weights
2	SCA	579	71	50	35	8	-	-	36	25
3	SCA	11	11	9	11	-	-	-	44	19
4	East of 170	323	54	50	44	8	-	-	44	13
5	SCA	494	61	61	50	13	-	-	12	12
6	SCA	356	71	54	46	4	-	-	67	20
7	East of 170	357	53	52	43	2	-	-	14	11
8	East of 170	386	68	63	47	6	-	-	32	10
9	East of 170	339	60	60	45	16	-	-	41	12
10	East of 170	320	53	51	43	6	-	-	44	10
11	East of 170	429	68	68	40	-	-	-	2	-
12	East of 170	305	50	50	40	3	-	-	87	27
13	East of 170	395	60	60	40	-	-	-	3	3
14	East of 170	343	56	56	46	6	-	-	5	5
15	West of 170	336	61	60	42	9	-	-	74	24
16	West of 170	444	50	50	50	-	-	-	1	-
17	West of 170	325	49	49	49	10	-	-	36	10
19	West of 170	345	50	50	50	9	-	-	32	10
21	West of 170	549	72	63	50	6	-	-	50	21
22	West of 170	359	57	56	57	15	-	-	3	3
23	West of 170	163	50	50	50	5	34	-	6	3
24	West of 170	457	61	61	50	6	-	-	56	30
25	West of 170	237	50	50	50	9	-	-	12	8
26	West of 170	11	11	11	11	-	11	-	12	12
27	West of 170	347	62	62	50	9	-	-	10	10
28	West of 170	385	50	50	50	6	-	-	40	29
29	West of 170	331	50	50	50	8	-	-	43	13
30	West of 170	392	50	50	49	5	-	-	46	14
31	West of 170	363	101	101	51	1	-	-	47	32
32	West of 170	471	68	60	55	6	-	-	67	24
33	West of 170	295	50	50	50	1	-	-	20	16
34	West of 170	361	52	52	50	3	-	-	17	10
35	West of 170	297	50	50	50	2	-	-	12	12
36	West of 170	351	50	50	50	1	-	-	31	13
37	West of 170	347	52	50	50	6	-	-	23	14
38	West of 170	319	51	50	51	4	-	-	14	10
39	West of 170	481	74	71	51	6	1	-	16	11
40	West of 170	325	50	50	50	1	-	-	46	29
41	West of 170	332	53	53	53	3	-	-	25	17
42	West of 170	351	54	54	50	1	-	-	63	20
43	West of 170	335	50	50	50	-	-	-	15	15

Haul	Region	Pollock age 1+					Pollock age 0		Other	
No.	Name	Lengths	Weights	Maturities	Otoliths	Ovaries	Lengths	Weights	Lengths	Weights
44	West of 170	354	51	51	50	3	-	-	14	14
45	West of 170	358	50	50	50	-	-	-	31	14
46	West of 170	336	50	50	50	-	-	-	28	18
47	West of 170	414	54	54	50	1	-	-	33	29
48	West of 170	424	61	60	51	-	-	-	14	14
49	EBS Northern Extension	5	5	1	5	-	50	-	55	28
50	EBS Northern Extension	15	15	15	15	6	20	-	49	15
51	EBS Northern Extension	1	1	1	1	-	9	-	10	6
52	EBS Northern Extension	3	3	3	3	2	40	-	92	33
53	EBS Northern Extension	2	2	2	2	1	25	-	30	17
54	EBS Northern Extension	39	28	8	13	3	25	-	50	27
55	EBS Northern Extension	91	32	12	17	6	25	-	40	27
56	EBS Northern Extension	9	9	5	9	-	25	-	1	1
57	EBS Northern Extension	2	2	2	2	1	30	-	93	30
58	EBS Northern Extension	51	51	51	30	3	26	-	10	9
59	EBS Northern Extension	9	9	9	9	2	25	-	54	29
60	EBS Northern Extension	85	50	50	30	-	-	-	38	14
61	EBS Northern Extension	5	5	5	5	-	-	-	46	14
62	EBS Northern Extension	254	50	50	30	-	-	-	39	9
63	EBS Northern Extension	180	50	50	30	2	-	-	44	12
65	EBS Northern Extension	46	46	46	31	3	-	-	47	13
66	EBS Northern Extension	319	50	50	30	12	2	-	42	11
67	EBS Cross Transect	313	50	50	30	9	29	-	42	14
68	EBS Cross Transect	416	65	60	35	10	10	-	43	22
69	EBS Cross Transect	391	50	50	30	8	9	-	23	13
70	EBS Cross Transect	329	50	50	30	7	10	-	13	13
71	EBS Cross Transect	366	50	50	30	3	25	-	39	15
72	EBS Cross Transect	301	50	50	30	2	31	-	15	15
73	EBS Cross Transect	306	54	49	34	2	25	-	23	14
75	EBS Cross Transect	32	32	32	30	-	25	-	47	19
Total		19,402	3,289	3,153	2,611	290	512	0	2,353	1,086

Table 10. -- Estimates of walleye pollock biomass (millions of metric tons) and relative estimation error for the core area of the Eastern Bering Sea. For 2020, results are from the saildrone survey, and 2018 includes the unsampled area.

			SCA		East of 170		West of 170		EBS	
Year	Dates	Area (nm^2)	Biomass	%	Biomass	%	Biomass	%	Biomass	Est. error
2004	4 Jun -29 Jul	99,659	0.550	13.8	0.918	23.0	2.528	63.3	3.996	3.1%
2006	3 Jun -25 Jul	89,550	0.147	7.5	0.340	17.5	1.456	74.9	1.943	3.3%
2007	2 Jun -30 Jul	92,944	0.136	6.0	0.245	10.7	1.902	83.3	2.283	3.8%
2008	2 Jun -31 Jul	95,374	0.122	8.7	0.087	6.2	1.196	85.1	1.404	5.6%
2009	9 Jun -7 Aug	91,414	0.156	11.7	0.058	4.4	1.117	83.9	1.331	6.9%
2010	5 Jun -7 Aug	92,849	0.098	3.7	0.193	7.3	2.345	89.0	2.636	5.4%
2012	7 Jun -10 Aug	96,852	0.196	8.6	0.319	14.0	1.764	77.4	2.279	3.4%
2014	12 Jun -13 Aug	94,361	0.571	12.0	1.458	30.7	2.714	57.2	4.743	3.4%
2016	12 Jun -17 Aug	100,674	0.542	11.2	1.268	26.2	3.028	62.6	4.838	1.9%
2018	12 Jun -22 Aug	92,283	0.234	9.4	0.510	20.4	1.753	70.2	2.497	3.9%
2020	4 Jul - 20 Aug	102,320	0.398	11.0	0.531	14.7	2.688	74.3	3.617	9.6%
2022	1 Jun -5 Aug	103,942	0.538	14.0	0.826	21.5	2.470	64.4	3.834	6.8%

Table 11. -- Numbers-at-length estimates (millions of fish) from acoustic-trawl surveys of walleye pollock in the core area of the Eastern Bering Sea.

Length	2004	2006	2007	2008	2009	2010	2012	2014	2016	2018	2022
10	<1	2.9	32.6	<1	48.9	<1	1.6	3.6	<1	<1	3.6
11	1.0	9.4	268.9	1.7	228.2	1.1	8.3	24.6	2.5	<1	7.8
12	4.9	65.0	680.2	5.0	779.8	9.5	13.7	95.2	6.8	2.7	14.8
13	7.4	151.1	1360.7	11.5	1127.7	68.7	16.4	511.5	19.1	10.2	20.5
14	14.2	127.7	1529.0	15.5	1103.3	267.0	24.9	966.9	28.3	26.1	28.0
15	11.2	93.1	824.7	10.5	1061.1	516.8	31.8	1183.0	34.3	55.8	21.8
16	12.2	33.1	577.9	6.4	543.3	807.9	25.0	964.2	24.9	95.7	13.4
17	9.7	11.6	310.6	7.8	270.3	705.0	14.7	585.8	18.8	98.0	12.4
18	6.0	4.2	117.8	47.7	85.7	305.6	9.3	306.3	12.0	96.1	9.7
19	7.7	5.5	135.3	128.2	84.6	155.9	24.8	106.3	19.6	39.6	8.2
20	11.5	11.8	118.4	265.7	57.8	175.2	77.5	73.2	33.3	18.5	9.0
21	26.2	18.1	145.0	410.0	79.4	227.5	188.5	105.1	70.9	11.7	13.0
22	39.2	33.0	147.4	447.2	109.3	372.9	312.8	213.3	139.3	19.4	19.9
23	52.3	38.7	129.6	566.5	138.0	625.7	388.2	442.9	179.4	36.7	22.2
24	53.7	35.6	143.3	446.2	114.5	934.3	356.2	1029.8	205.6	66.3	29.9
25	43.4	31.1	92.6	353.1	117.1	1165.5	289.5	1745.3	160.5	93.0	30.3
26	35.9	26.4	66.5	231.4	116.7	1171.4	223.7	1992.6	128.6	130.4	34.7
27	29.3	23.6	51.4	115.1	132.3	929.4	191.7	1536.7	118.8	109.0	36.6
28	32.4	27.1	34.9	79.3	143.3	578.8	206.2	959.7	148.3	91.7	45.0
29	72.7	31.6	22.9	101.5	186.6	274.2	260.9	494.1	175.6	48.1	82.1
30	93.7	37.3	20.1	129.8	210.4	131.9	304.1	328.6	294.9	23.2	101.7
31	153.3	44.1	17.2	125.1	258.0	89.8	279.5	220.2	468.5	17.1	162.8
32	154.6	48.1	36.2	134.8	249.2	104.0	228.3	167.1	634.0	17.8	222.6
33	182.5	54.8	47.4	120.3	203.0	114.4	192.6	152.9	751.3	25.5	360.5
34	187.3	73.5	62.7	117.5	157.3	129.4	210.8	122.8	731.7	31.0	565.2
35	239.8	88.2	76.8	88.3	110.4	163.1	261.5	170.3	697.7	53.8	764.8
36	305.3	120.0	66.9	46.1	88.7	235.6	338.3	189.8	534.4	93.4	908.2
37	433.1	129.2	84.0	32.5	65.9	292.5	411.1	247.2	433.9	165.4	977.1
38	483.7	139.3	81.4	28.3	47.4	391.7	446.9	265.7	502.9	236.7	1049.0
39	549.4	132.3	90.9	36.8	42.6	416.8	406.5	282.1	732.8	320.7	913.2
40	522.2	147.4	118.6	31.1	35.1	382.4	349.1	248.9	1011.9	425.0	776.6
41	540.2	165.6	129.0	33.8	30.6	299.2	232.4	250.5	992.0	496.3	612.2
42	523.3	187.5	165.9	43.5	29.7	218.5	159.6	274.1	751.5	516.6	433.4
43	507.5	199.0	219.6	50.2	26.6	147.6	98.4	390.9	493.0	488.6	303.9
44	455.6	218.8	228.2	63.2	21.1	103.8	90.7	415.0	354.2	376.7	207.0
45	404.6	209.6	259.6	66.1	26.2	71.0	81.1	480.8	271.4	299.3	118.4
46	320.2	200.9	260.0	86.1	26.2	51.4	87.3	428.2	210.8	239.5	97.1
47	262.4	180.8	231.3	83.7	29.2	32.8	83.5	364.6	176.0	180.5	89.3
48	219.3	168.6	198.7	97.7	40.9	20.5	79.9	271.1	153.4	141.5	83.8
49	181.7	131.9	172.5	78.2	44.8	17.5	66.4	215.4	126.1	107.0	81.1
50	140.7	118.1	144.5	74.3	43.4	19.2	55.5	152.9	108.7	71.0	78.1
51	116.1	93.2	109.9	70.5	43.3	17.4	40.0	122.8	78.8	53.7	68.7
52	102.8	83.2	90.2	61.1	43.4	16.9	35.7	90.9	59.1	38.4	66.1
53	80.5	60.3	67.6	46.6	38.3	16.3	26.4	70.0	43.1	26.2	43.4
54	65.4	49.0	60.8	43.9	38.0	19.1	26.5	50.3	30.8	16.7	39.9
55	43.0	33.8	41.3	34.8	33.0	15.5	17.9	40.2	20.4	12.9	30.6
56	34.2	29.4	31.0	27.6	25.2	15.7	15.9	29.2	14.6	8.7	19.3
57	23.6	22.8	25.5	21.7	19.7	15.8	13.5	26.5	12.0	5.4	12.9
58	16.1	17.7	15.8	18.1	20.4	14.8	13.8	22.1	6.1	4.2	6.1
59	13.8	13.0	11.3	17.0	13.6	9.8	11.4	20.5	4.4	2.4	5.2
60	9.4	9.1	9.0	13.8	11.3	11.8	12.1	14.9	3.5	1.5	4.8
61	7.6	7.7	5.5	8.1	9.4	10.3	9.2	13.1	2.4	1.5	1.8
62	4.8	4.5	4.9	9.2	8.6	7.9	9.5	9.6	2.4	<1	1.2
63	4.1	3.1	3.6	5.7	5.0	5.5	5.9	7.4	2.3	<1	<1
64	1.2	3.7	3.3	4.4	5.1	5.6	7.0	4.6	1.4	<1	1.1
65	1.0	1.6	2.0	3.1	5.3	3.5	4.1	4.8	1.2	<1	<1
66	1.2	1.7	1.8	2.4	4.1	3.3	4.2	2.7	<1	<1	<1
67	<1	<1	1.3	1.7	2.9	2.3	2.1	1.4	1.3	<1	<1
68	<1	<1	<1	1.5	1.9	2.5	2.4	1.2	<1	<1	<1
69	<1	<1	<1	<1	1.8	<1	<1	1.2	<1	<1	<1
70	<1	<1	<1	<1	1.3	<1	1.3	1.2	<1	<1	<1
Total	7,858.59	4,011.35	9,987.59	5,210.74	8,646.03	12,921.00	7,389.38	19,513.85	12,243.94	5,551.42	9,673.05

Table 12. -- Biomass-at-length estimates (thousands of metric tons) from acoustic-trawl surveys of walleye pollock in the core area of the Eastern Bering Sea

Length	2004	2006	2007	2008	2009	2010	2012	2014	2016	2018	2022
5	<1	<1	<1	<1	<1	<1	<1	<1	<1	<1	0
6	<1	<1	<1	<1	<1	<1	<1	<1	<1	<1	0
7	<1	<1	<1	<1	<1	<1	<1	<1	<1	<1	0
8	<1	<1	<1	<1	<1	<1	<1	<1	<1	<1	0
9	<1	<1	<1	<1	<1	<1	<1	<1	<1	<1	<1
10	<1	<1	<1	<1	<1	<1	<1	<1	<1	<1	<1
11	<1	<1	2.5	<1	2.1	<1	<1	<1	<1	<1	<1
12	<1	<1	7.5	<1	9.3	<1	<1	1.1	<1	<1	<1
13	<1	2.5	19.5	<1	17.4	1.1	<1	7.9	<1	<1	<1
14	<1	2.3	26.3	<1	21.9	5.6	<1	18.1	<1	<1	<1
15	<1	2.2	18.2	<1	26.0	13.2	<1	27.8	<1	1.2	<1
16	<1	<1	15.2	<1	16.4	25.4	<1	27.3	<1	2.6	<1
17	<1	<1	10.1	<1	10.3	26.4	<1	19.8	<1	3.1	<1
18	<1	<1	4.5	1.8	3.7	13.4	<1	12.4	<1	3.8	<1
19	<1	<1	6.3	5.9	4.3	7.6	1.2	4.9	<1	1.8	<1
20	<1	<1	6.4	14.1	3.3	10.0	4.1	4.0	1.7	<1	<1
21	1.8	1.2	9.8	25.1	5.4	15.4	11.7	6.6	4.3	<1	<1
22	3.0	2.5	11.6	32.5	8.8	29.6	22.3	16.0	10.0	1.4	1.4
23	4.7	3.4	11.5	47.9	12.5	56.5	32.8	40.6	14.4	3.1	1.8
24	5.4	3.4	14.6	42.8	11.7	97.0	34.3	108.3	19.4	6.1	2.7
25	4.9	3.3	10.3	38.1	14.3	137.2	31.3	209.9	16.9	10.0	3.1
26	4.7	3.3	8.1	28.1	15.7	154.0	27.1	270.0	15.3	15.9	4.1
27	4.3	3.2	7.0	15.7	20.8	136.3	26.3	231.3	16.2	15.2	4.9
28	5.3	4.1	5.3	12.0	24.3	95.7	31.4	157.5	22.6	14.2	6.6
29	13.2	5.3	3.9	17.0	36.8	49.7	44.9	89.8	29.6	8.5	13.8
30	18.6	6.9	3.8	23.9	45.0	25.4	57.0	65.4	54.3	4.4	19.2
31	33.6	9.6	3.6	25.8	61.7	19.6	59.2	47.4	97.3	3.6	33.6
32	37.0	11.4	8.8	30.4	64.9	25.0	52.5	39.7	146.4	4.1	51.0
33	48.8	14.1	12.4	30.0	57.8	30.7	48.0	39.8	189.9	6.4	91.1
34	54.0	20.5	18.0	31.3	48.4	38.6	57.3	34.9	202.5	8.6	153.4
35	74.7	26.8	24.0	26.4	36.7	53.0	77.1	53.4	211.6	16.2	223.9
36	104.2	39.5	22.5	15.1	31.6	83.1	108.9	65.5	178.2	31.6	291.6
37	157.8	44.9	31.0	11.5	24.6	111.6	144.3	91.8	158.3	60.1	341.2
38	190.7	53.0	32.4	10.8	19.5	163.8	166.5	106.8	205.1	92.8	395.2
39	233.1	54.6	38.9	15.1	18.2	185.0	163.5	121.2	327.7	134.5	378.3
40	240.1	64.6	53.7	13.9	16.2	183.8	151.4	115.3	490.6	189.9	348.4
41	265.6	77.4	62.4	16.0	15.5	153.4	107.9	124.9	514.1	235.2	295.0
42	276.3	95.0	84.9	21.5	16.1	119.1	79.5	145.5	410.5	263.3	222.9
43	290.7	106.2	121.6	27.3	15.4	85.5	52.3	222.5	281.1	265.7	162.4
44	278.1	126.1	133.3	36.2	13.0	63.9	51.4	250.5	212.3	219.5	117.3
45	261.4	127.2	162.4	40.5	16.6	46.2	49.4	308.0	170.8	186.9	68.6
46	217.5	129.4	174.5	55.6	18.3	35.9	56.3	290.9	138.2	156.5	60.0
47	188.4	123.8	163.2	57.7	21.6	24.0	58.1	261.8	119.7	124.4	59.1
48	164.4	121.3	149.7	69.8	32.3	16.3	59.5	205.4	110.9	101.5	58.1
49	143.7	100.8	136.0	60.1	37.0	14.6	52.2	172.2	95.6	81.1	59.4
50	117.9	97.4	121.9	60.9	38.5	16.9	45.7	129.1	86.2	56.5	61.0
51	102.8	79.9	97.2	60.0	40.2	16.4	35.4	110.6	66.0	44.5	56.8
52	95.2	74.8	84.9	56.3	42.9	16.7	32.6	87.2	51.9	32.9	59.3
53	79.2	58.4	66.1	46.0	39.2	16.8	26.3	70.1	39.6	24.2	41.7
54	67.7	50.0	64.6	44.8	41.5	20.9	27.8	53.4	30.2	16.1	39.1
55	46.3	36.4	46.6	38.2	37.7	17.8	19.9	45.0	21.5	13.3	31.7
56	39.5	32.2	36.6	32.9	30.8	19.4	18.1	34.3	15.8	9.6	21.4
57	29.0	26.9	32.1	26.6	26.0	19.9	16.4	32.3	13.9	6.4	14.8
58	20.1	22.3	20.6	24.0	27.3	19.8	17.6	28.7	7.5	5.2	7.4
59	18.9	17.2	15.9	23.0	20.0	14.2	14.8	28.5	5.9	3.1	6.9
60	13.4	13.1	13.2	20.5	17.3	18.1	17.2	21.5	4.7	2.0	6.8
61	11.7	11.3	8.4	12.5	15.2	16.7	13.5	19.8	3.6	2.1	2.6
62	7.5	7.0	7.8	15.2	14.2	13.1	15.0	15.8	3.7	1.1	1.9
63	6.9	5.0	6.3	9.6	8.8	9.6	9.6	12.2	3.8	1.1	<1
64	2.1	6.2	5.9	7.5	9.3	10.4	11.9	8.2	2.4	1.1	1.8
65	1.8	2.9	3.7	5.6	10.2	6.9	7.5	8.7	2.2	1.0	<1
66	2.3	3.2	3.6	4.5	8.2	7.0	7.9	5.5	1.3	<1	<1
67	1.4	1.4	2.6	3.5	6.1	4.9	4.2	2.8	2.7	<1	1.1
68	1.2	1.0	1.8	3.1	4.1	5.8	4.9	2.7	<1	<1	<1
69	<1	<1	<1	1.3	4.2	1.7	1.9	2.5	1.7	<1	<1
70	<1	<1	2.3	1.7	3.1	2.2	2.9	2.9	<1	<1	2.0
71	<1	<1	1.2	<1	2.0	<1	1.4	<1	<1	<1	0
72	<1	1.2	<1	1.8	1.9	1.8	1.1	1.6	<1	<1	1.6
73	<1	<1	<1	<1	1.7	2.6	<1	<1	<1	<1	<1
74	<1	<1	<1	<1	1.4	1.1	1.3	<1	<1	<1	<1
75	<1	<1	<1	<1	1.6	<1	<1	<1	<1	<1	0
76	<1	<1	<1	<1	<1	<1	<1	<1	<1	<1	<1

Length	2004	2006	2007	2008	2009	2010	2012	2014	2016	2018	2022
77	<1	<1	<1	<1	<1	<1	<1	<1	<1	<1	<1
78	<1	<1	<1	<1	<1	<1	<1	<1	<1	<1	0
79	<1	<1	<1	<1	<1	<1	<1	<1	<1	<1	0
80	<1	<1	<1	<1	<1	<1	<1	<1	<1	<1	0
81	<1	<1	<1	<1	<1	<1	<1	<1	<1	<1	0
82	<1	<1	<1	<1	<1	<1	<1	<1	<1	<1	0
83	<1	<1	<1	<1	<1	<1	<1	<1	<1	<1	0
84	<1	<1	<1	<1	<1	<1	<1	<1	<1	<1	0
85	<1	<1	<1	<1	<1	<1	<1	<1	<1	<1	0
86	<1	<1	<1	<1	<1	<1	<1	<1	<1	<1	0
87	<1	<1	<1	<1	<1	<1	<1	<1	<1	<1	0
88	<1	<1	<1	<1	<1	<1	<1	<1	<1	<1	0
89	<1	<1	<1	<1	<1	<1	<1	<1	<1	<1	0
90	<1	<1	<1	<1	<1	<1	<1	<1	<1	<1	0
91	<1	<1	<1	<1	<1	<1	<1	<1	<1	<1	0
92	<1	<1	<1	<1	<1	<1	<1	<1	<1	<1	0
93	<1	<1	<1	<1	<1	<1	<1	<1	<1	<1	0
94	<1	<1	<1	<1	<1	<1	<1	<1	<1	<1	0
95	<1	<1	<1	<1	<1	<1	<1	<1	<1	<1	0
Total	3995.7	1943.4	2282.7	1404.5	1331.4	2635.7	2279.4	4742.8	4837.7	2497.3	3834.0

Table 13. --Numbers-at-age estimates (millions of fish) from acoustic-trawl surveys of walleye pollock in the core area of the Eastern Bering Sea.

Age	2004	2006	2007	2008	2009	2010	2012	2014	2016	2018	2022
1	67.8	501.8	5726.2	57.4	5207.8	2560.8	145.1	4697.3	163.1	411.8	141.6
2	314.8	217.2	1034.5	2901.0	818.2	6377.3	1954.5	8704.4	1037.6	521.8	332.3
3	1218.3	298.1	339.4	1053.0	1742.6	978.1	1663.8	966.8	4501.3	254.5	975.2
4	3106.7	677.3	473.0	165.4	285.0	2288.1	2705.1	1146.1	4499.6	606.7	6577.7
5	1624.9	822.2	791.7	156.7	76.1	448.2	282.3	1105.8	719.3	2295.2	819.4
6	567.8	686.3	734.5	282.0	92.6	74.0	371.2	1805.3	348.1	951.6	211.0
7	288.5	407.5	412.0	235.2	130.2	33.1	114.3	758.3	398.1	200.3	133.0
8	283.6	150.4	245.3	138.5	112.0	36.4	35.6	169.5	427.8	112.0	239.1
9	122.8	77.2	98.8	103.1	77.3	38.0	24.0	76.8	94.3	102.7	166.3
10	69.0	60.7	39.4	32.9	44.6	29.1	27.6	29.5	28.9	69.7	33.9
11	58.9	33.8	37.4	30.2	26.0	25.9	23.8	11.1	15.9	17.1	16.7
12	77.5	22.4	19.4	19.6	11.2	13.2	16.9	11.9	4.4	4.9	17.9
13	37.0	16.5	8.9	10.7	10.1	7.9	14.9	11.7	2.4	2.6	6.6
14	11.8	20.0	9.3	5.6	5.1	4.7	4.6	6.5	1.4	0	2.1
15	8.9	10.0	10.2	5.8	3.7	3.2	3.5	5.5	2.3	<1	1.6
16	<1	6.6	4.7	7.8	3.4	1.2	1.4	3.6	<1	<1	0
17	<1	2.0	<1	3.6	2.5	<1	<1	2.7	<1	0	0
18	<1	<1	1.5	1.6	2.3	2.0	<1	1.6	<1	<1	0
19	<1	2.6	1.0	2.4	1.6	<1	<1	<1	<1	<1	0
20	<1	<1	<1	<1	2.3	<1	<1	<1	<1	<1	0
21	<1	<1	<1	<1	<1	<1	<1	<1	<1	<1	0
22	<1	<1	<1	<1	<1	<1	<1	<1	<1	<1	0
23	<1	<1	<1	<1	<1	<1	<1	<1	<1	<1	0
24	<1	<1	<1	<1	<1	<1	<1	<1	<1	<1	0
25	<1	<1	<1	<1	<1	<1	<1	<1	<1	<1	0
26	<1	<1	<1	<1	<1	<1	<1	<1	<1	<1	0
27	<1	<1	<1	<1	<1	<1	<1	<1	<1	<1	0
28	<1	<1	<1	<1	<1	<1	<1	<1	<1	<1	0
29	<1	<1	<1	<1	<1	<1	<1	<1	<1	<1	0
Total	7859.7	4013.2	9989.5	5213.0	8655.4	12923.8	7392.5	19516.3	12244.8	5551.9	9674.4

Table 14. -- Biomass-at-age estimates (thousands of tons) from acoustic-trawl surveys of walleye pollock in the core area of the Eastern Bering Sea.

Age	2004	2006	2007	2008	2009	2010	2012	2014	2016	2018	2022
1	1.7	9.6	105.6	1.2	105.8	80.9	2.9	118.1	4.4	12.7	3.2
2	35.9	21.9	90.4	241.6	80.0	748.3	181.4	1172.0	106.3	60.3	54.2
3	338.2	72.2	95.4	227.1	417.2	216.9	340.0	218.1	1198.4	57.3	273.9
4	1440.7	257.3	209.4	67.9	121.3	1015.6	1027.7	453.8	2176.7	240.7	2481.9
5	932.0	435.0	463.9	90.2	46.5	259.3	158.9	608.1	381.9	1173.3	389.5
6	397.8	445.5	512.5	196.9	74.2	56.2	272.5	1244.7	218.2	568.6	120.0
7	223.8	310.0	330.8	191.8	121.5	33.6	96.8	565.4	280.5	132.2	97.5
8	239.2	127.2	217.9	131.2	116.2	42.5	35.7	164.4	331.0	82.4	192.0
9	113.7	71.9	96.3	100.6	85.7	47.6	29.8	81.5	76.8	82.1	139.7
10	66.6	60.0	43.0	38.6	55.5	39.4	35.5	34.0	28.5	61.9	32.4
11	59.6	34.4	41.6	37.0	33.9	35.8	30.9	15.1	18.5	16.3	18.0
12	80.5	26.1	22.8	23.8	16.8	19.9	22.7	16.5	6.0	4.9	17.8
13	39.5	20.2	11.7	14.7	16.4	13.2	21.5	18.0	3.7	2.7	8.0
14	13.6	25.2	13.3	8.3	9.0	8.2	7.6	9.7	2.3	<1	2.9
15	11.3	12.2	13.4	8.1	6.1	5.8	5.8	8.8	3.8	<1	3.1
16	1.3	8.0	6.6	12.2	6.6	2.3	2.6	5.3	<1	<1	0
17	<1	2.8	1.9	5.5	5.1	2.0	1.7	3.9	<1	<1	0
18	<1	<1	2.5	3.1	4.7	4.4	<1	2.2	<1	<1	0
19	<1	3.1	1.9	3.6	3.0	1.9	1.6	1.3	<1	<1	0
20	<1	<1	<1	<1	3.6	<1	<1	<1	<1	<1	0
21	<1	<1	<1	<1	1.5	<1	1.6	<1	<1	<1	0
22	<1	<1	<1	<1	<1	<1	<1	<1	<1	<1	0
23	<1	<1	<1	<1	<1	<1	<1	<1	<1	<1	0
24	<1	<1	<1	<1	<1	<1	<1	0	<1	<1	0
25	<1	<1	<1	<1	<1	<1	<1	<1	<1	<1	0
26	<1	<1	<1	<1	<1	<1	<1	<1	<1	<1	0
27	<1	<1	<1	<1	<1	<1	<1	<1	<1	<1	0
28	<1	<1	<1	<1	<1	<1	<1	<1	<1	<1	0
29	<1	<1	<1	<1	<1	<1	<1	<1	<1	<1	0
Total	3995.71	1943.42	2282.66	1404.47	1331.39	2635.73	2279.43	4742.84	4837.7	2497.29	3834.04

FIGURES

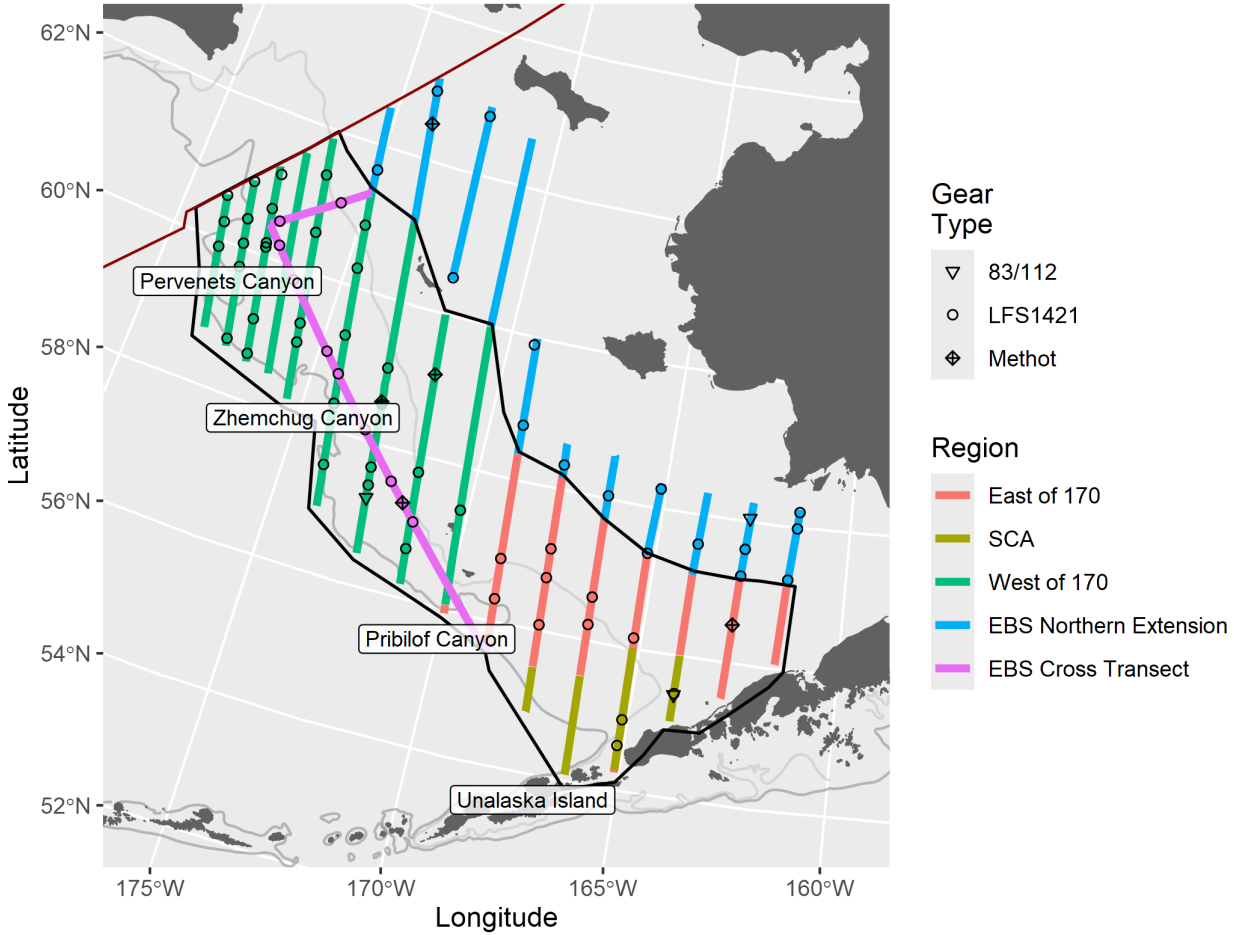

Figure 1. -- Transect lines and locations of trawl hauls during the 2022 eastern Bering Sea acoustic-trawl survey. The survey region associated with each transect is indicated by the transect color. The location of trawl events are indicated with black markers. Transects within the Steller sea lion conservation area (SCA; shown in khaki) are part of the region east of 170° W, and included in summaries of that region. Together, east of 170° W (including the SCA) and west of 170° W comprise the "core area", outlined in black on the map.

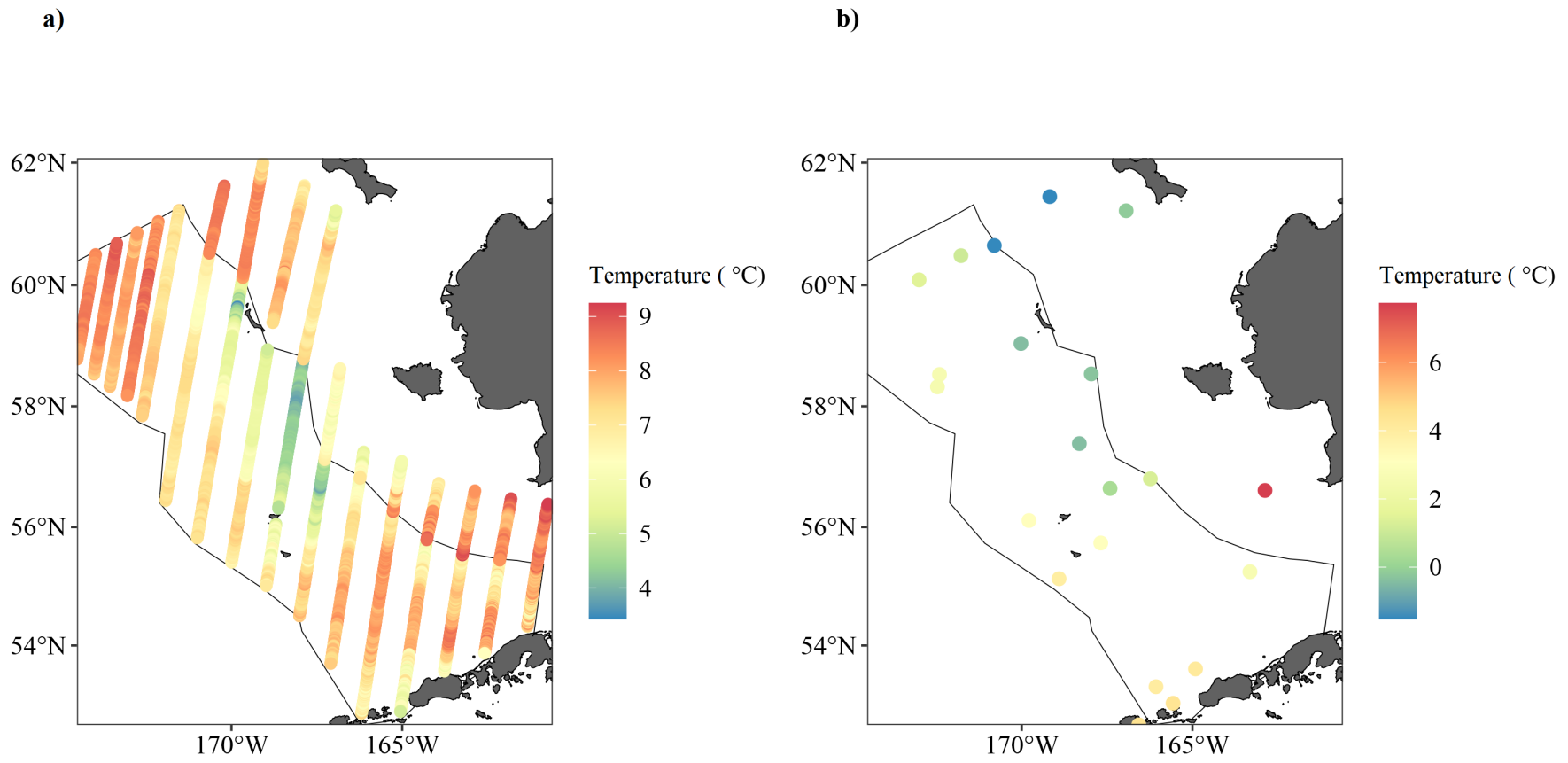

Figure 2. -- Water temperatures (° C) recorded at a) the sea surface at 5-second intervals from the ship's sea surface temperature system and b) near bottom during 23 conductivity-temperature-depth (CTD) casts during the summer 2022 acoustic-trawl survey of the eastern Bering Sea. Three of the CTD casts were conducted in Captains Bay, Unalaka, just southwest of the core area, and were associated with acoustic system calibrations. The core area is outlined in black, and the northern extension is to the north of the core area. Note that temperature color scales differ between plots.

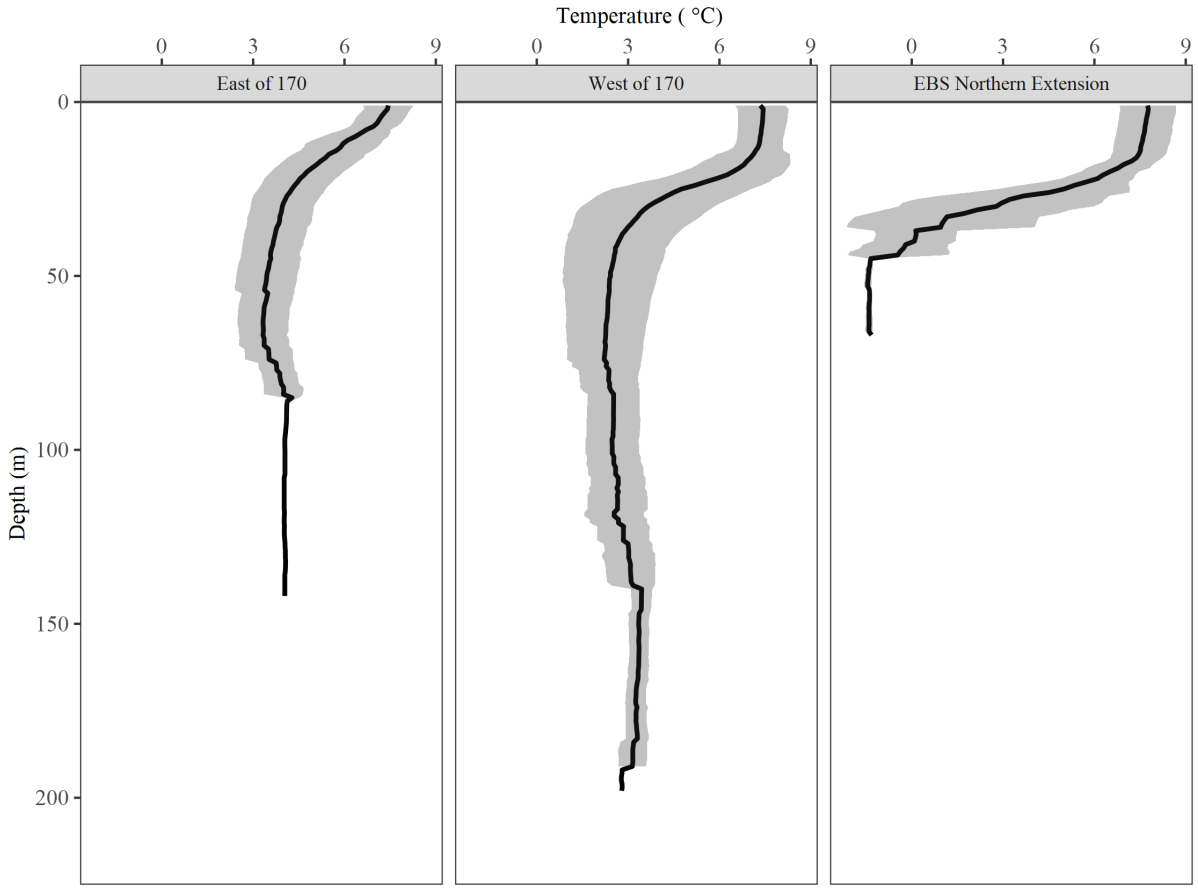

Figure 3. -- Temperature profiles at fishing locations from SBE-39 probes placed on the headrope of fishing gear in the core area (East and West of 170° W) and northern extension. Black line represents the mean and the gray ribbon represents 1 S.D. East of 170° W includes the Steller sea lion conservation area (SCA).

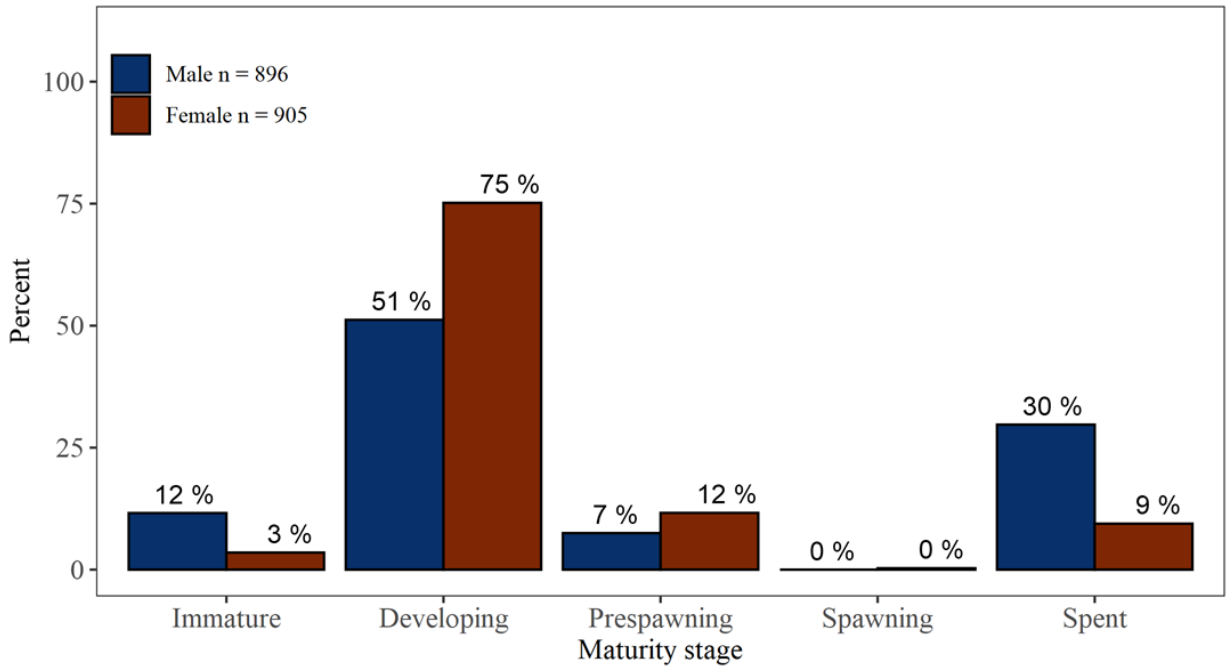

Figure 4. -- Maturity composition for male and female pollock ≥ 34 cm FL within each stage in the 2022 acoustic-trawl survey of the core area of the eastern Bering Sea. Maturity quantities are weighted by local pollock abundance.

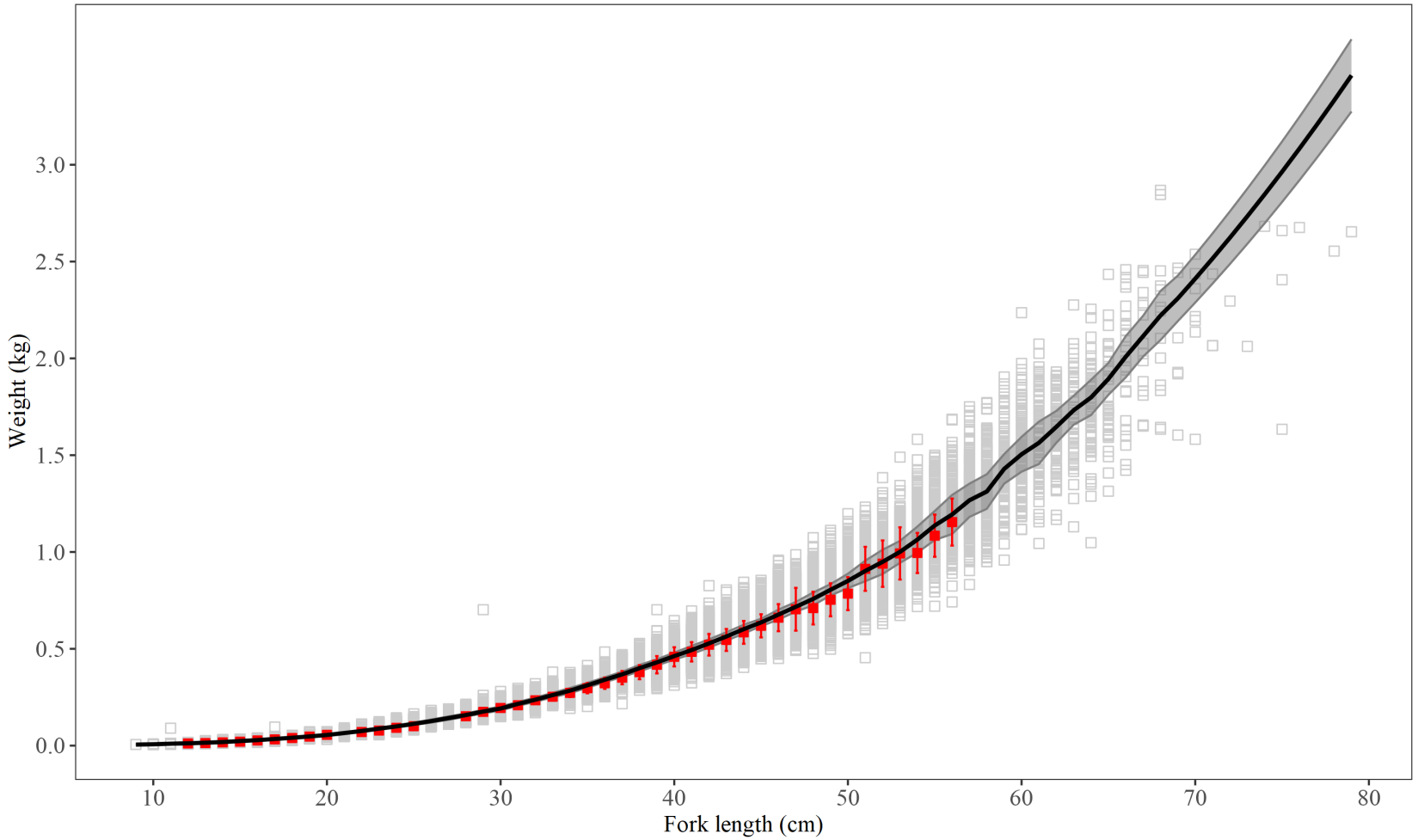

Figure 5. -- Pollock mean weight-at-length for pollock weighed during the AT survey of the eastern Bering Sea core area. The 2022 survey is highlighted in red (mean +/- 1 S.D.). Grey squares indicate the range of observations in previous surveys (2004-2018), and the black line and grey ribbon indicate mean weight-at-length in previous surveys +/- 1 S.D.

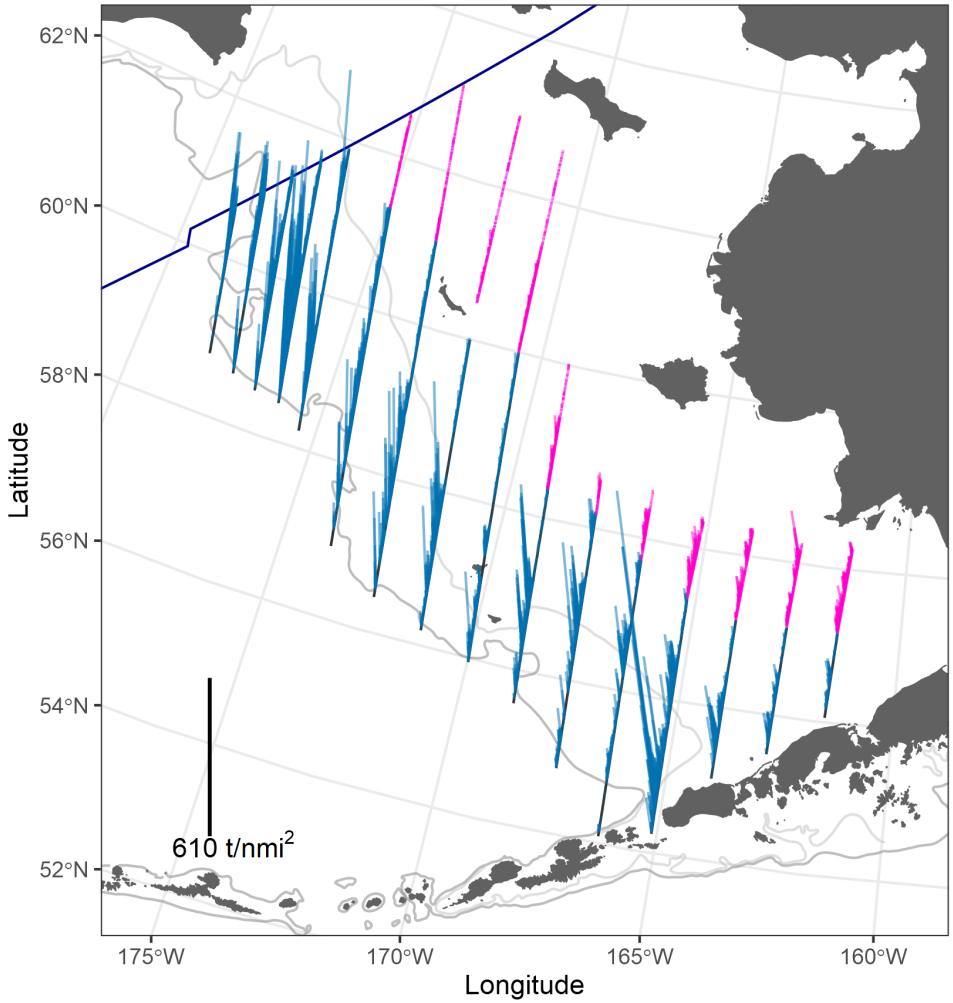

Figure 6. -- Density (t nmi^{-2}) attributed to pollock (vertical lines) along tracklines surveyed during the summer 2022 eastern Bering Sea acoustic-trawl survey of the core area (blue) and northern extension (pink).

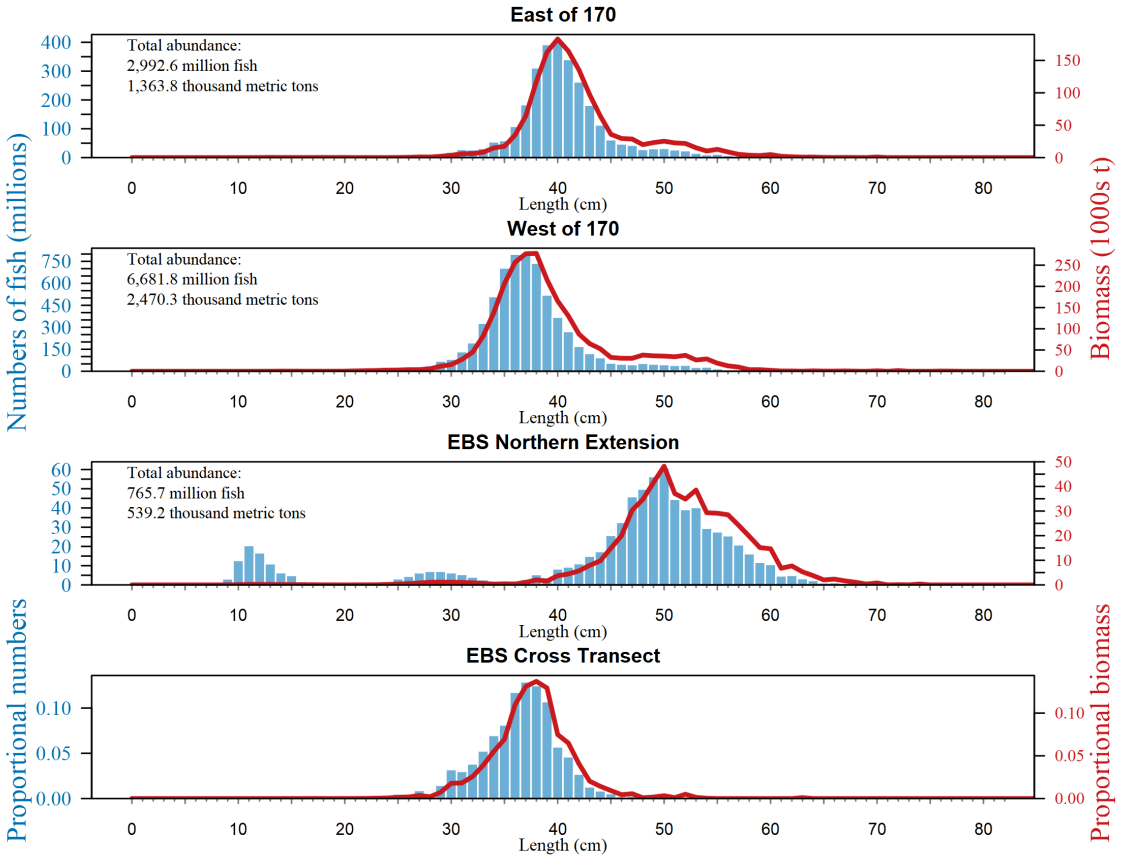

Figure 7. -- Pollock biomass (thousand metric tons; red line) and numbers (million fish; blue bars) at-length for the 2022 acoustic-trawl survey of the eastern Bering Sea. The core survey area and the Northern Extension include biomass and numbers-at-length down to 0.5 m off bottom. The cross-transect plot includes biomass and numbers down to 3 m off-bottom, shown as proportion of total biomass based on nearest haul applications.

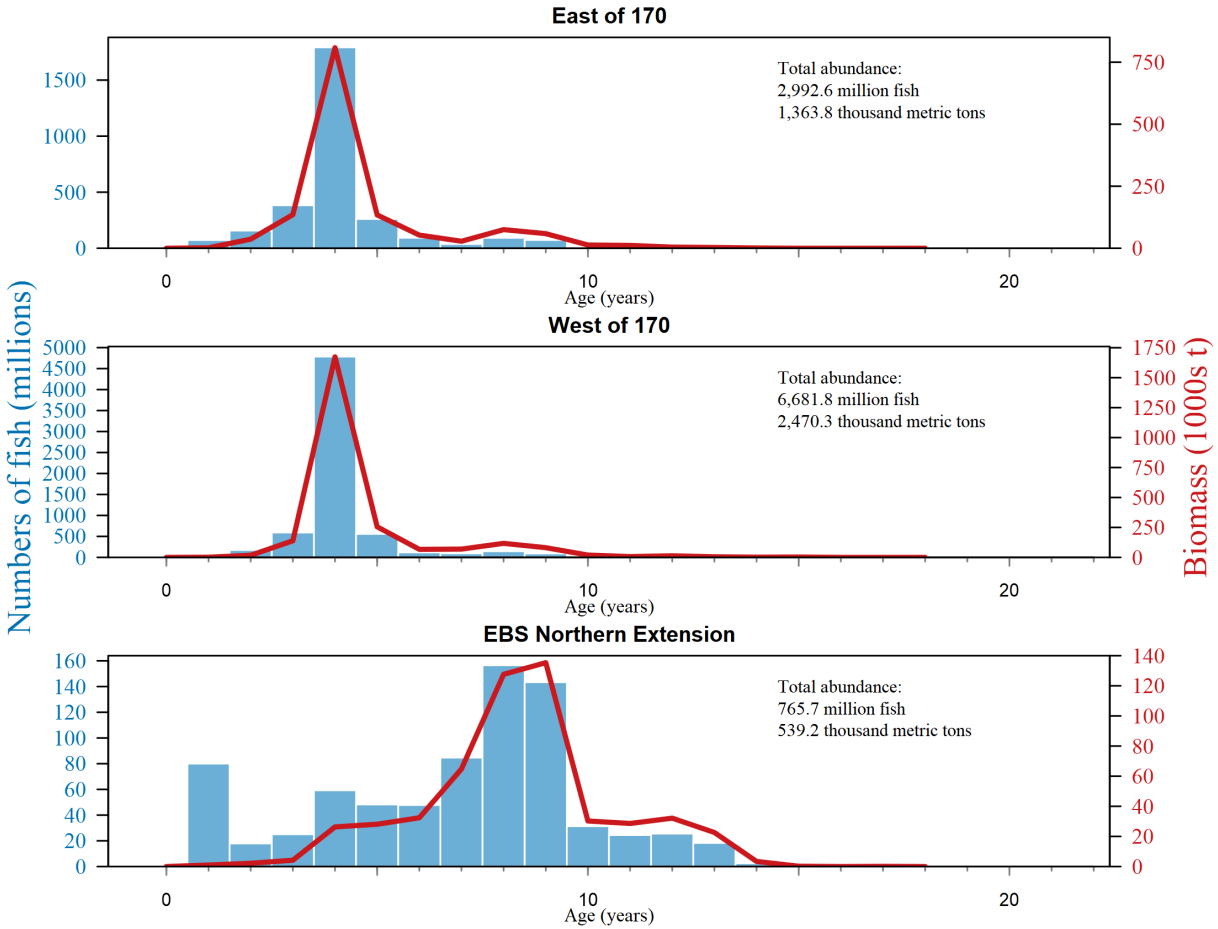

Figure 8. -- Pollock biomass (thousand metric tons; red line) and numbers (million fish; blue bars) at-age for the 2022 acoustic-trawl survey of the eastern Bering Sea.

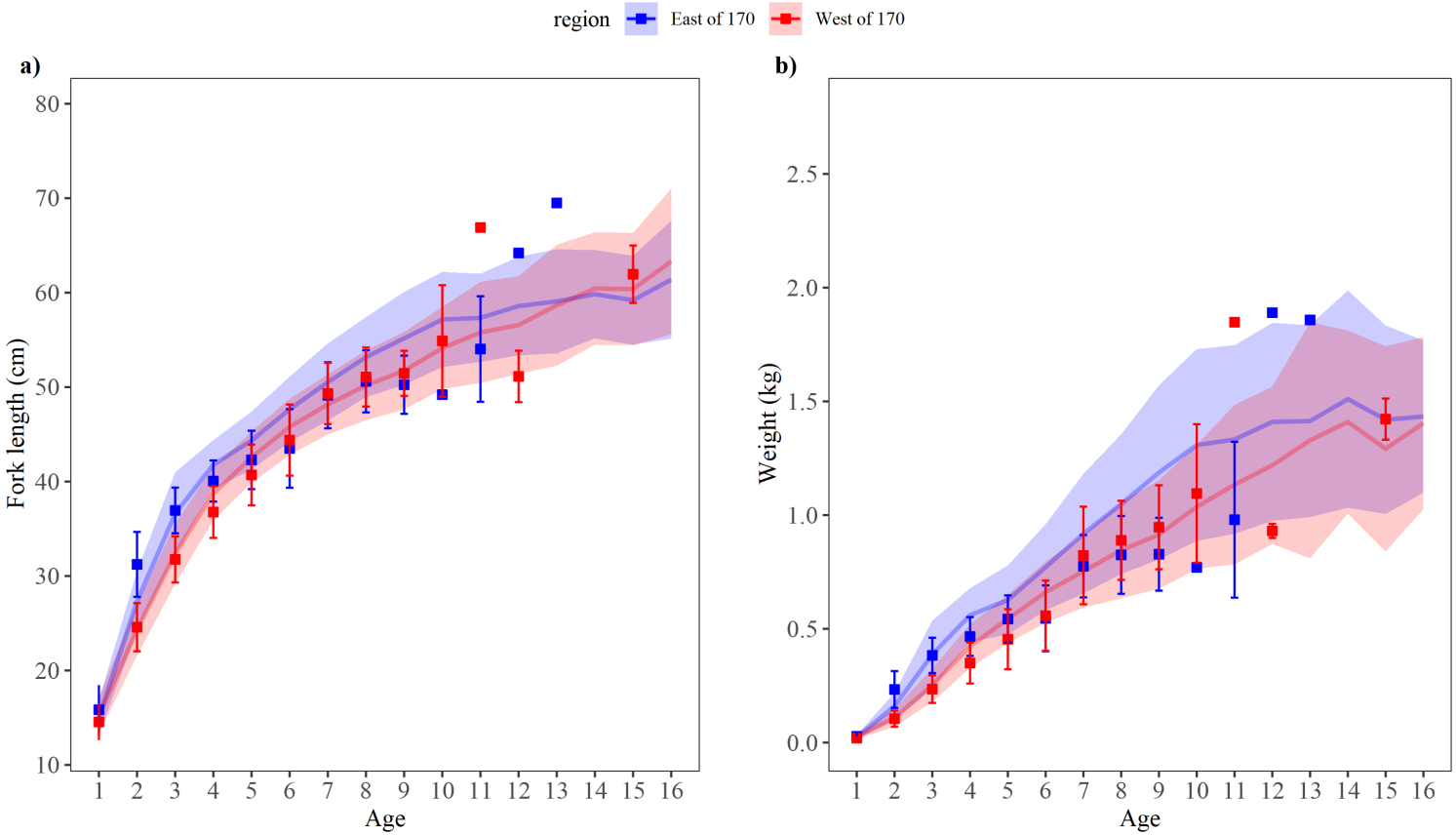

Figure 9. -- Pollock mean length-at-age for fish sampled in the acoustic trawl survey of the core area during summer eastern Bering Sea surveys. The mean length and weight-at-age of pollock found east of 170° W (including the Steller sea lion conservation area (SCA)) during the 2022 survey are depicted by blue squares, and mean length and weight-at-age of pollock found west of 170° W are depicted with red squares. Error bars represent mean +/- 1 S.D. The solid lines and shaded regions indicate the mean and +/- 1 S.D., respectively, for observations from 2004 to 2018. East of 170° W (blue) and west of 170° W (red) ribbons indicate mean length-at-age in historical surveys +/- 1 S.D.

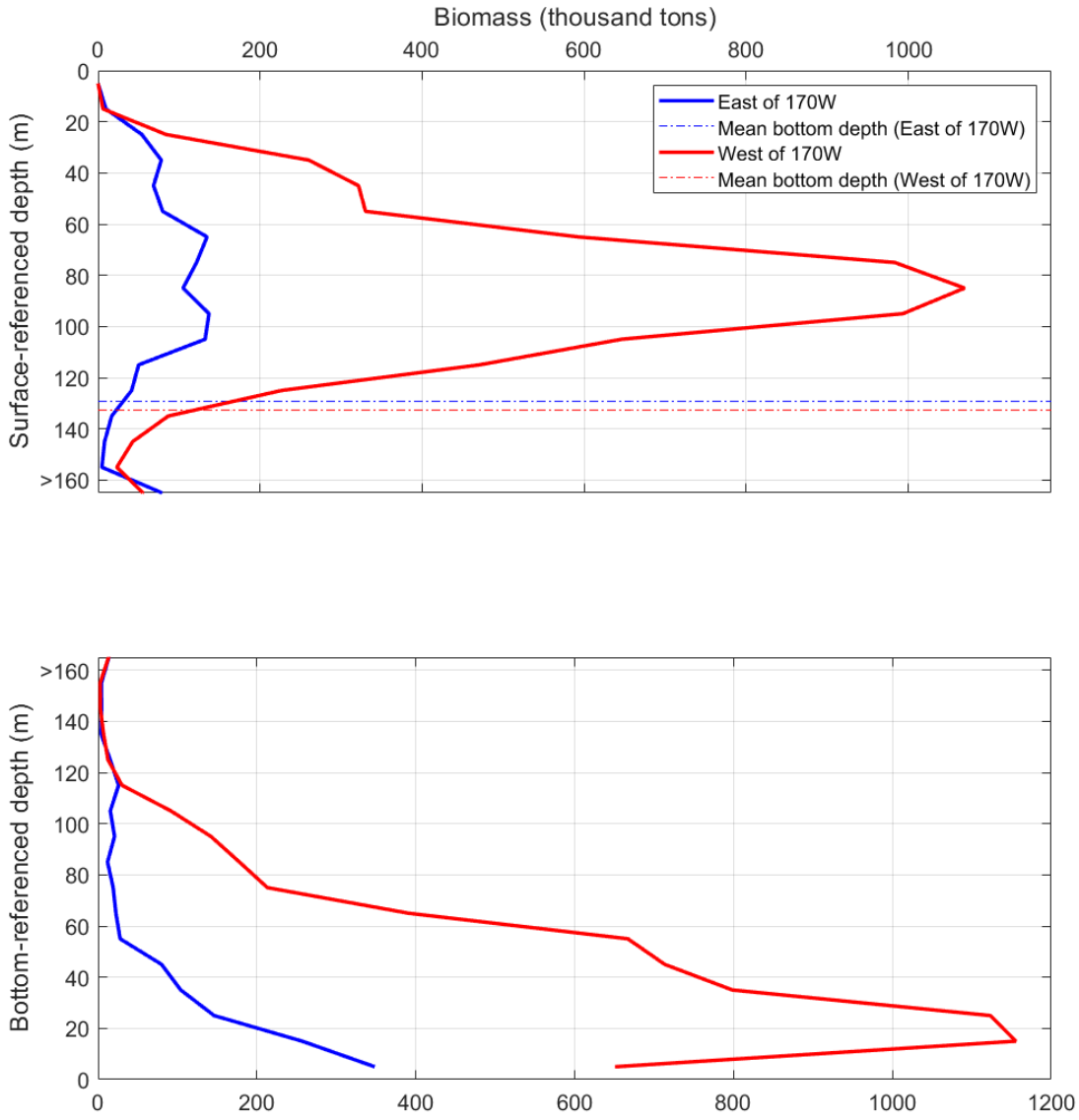

Figure 10. -- Depth distribution (m) of adult (≥ 30 cm FL) or juvenile (< 30 cm FL) walleye pollock biomass (thousand metric tons) east and west of 170° W longitude in the core survey area for the 2022 eastern Bering Sea shelf acoustic-trawl survey. Depth is referenced to the surface (upper panel) and to the bottom (lower panel). Data were averaged in 10 m depth bins from near surface to within 0.5 m of the seafloor.

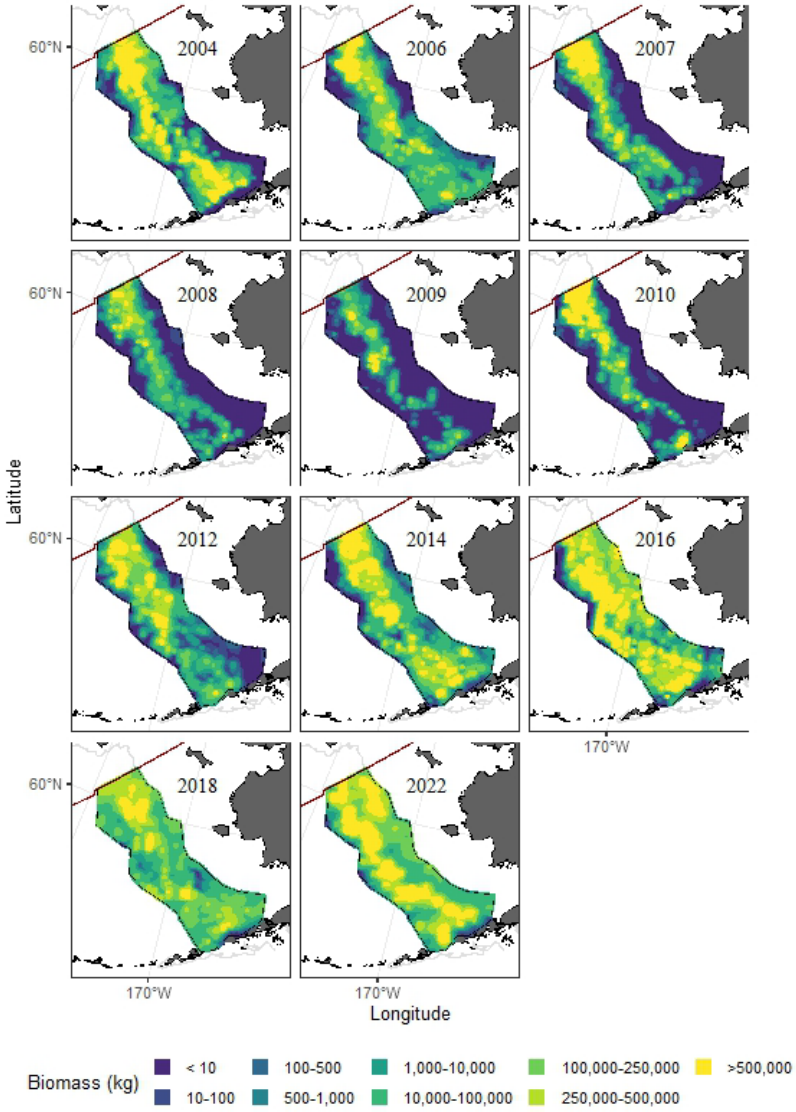

Figure 11. -- Walleye pollock biomass between near surface and 3 m off bottom in the U.S. core area for summer eastern Bering Sea shelf acoustic-trawl surveys of the core area between 2004 and 2022.

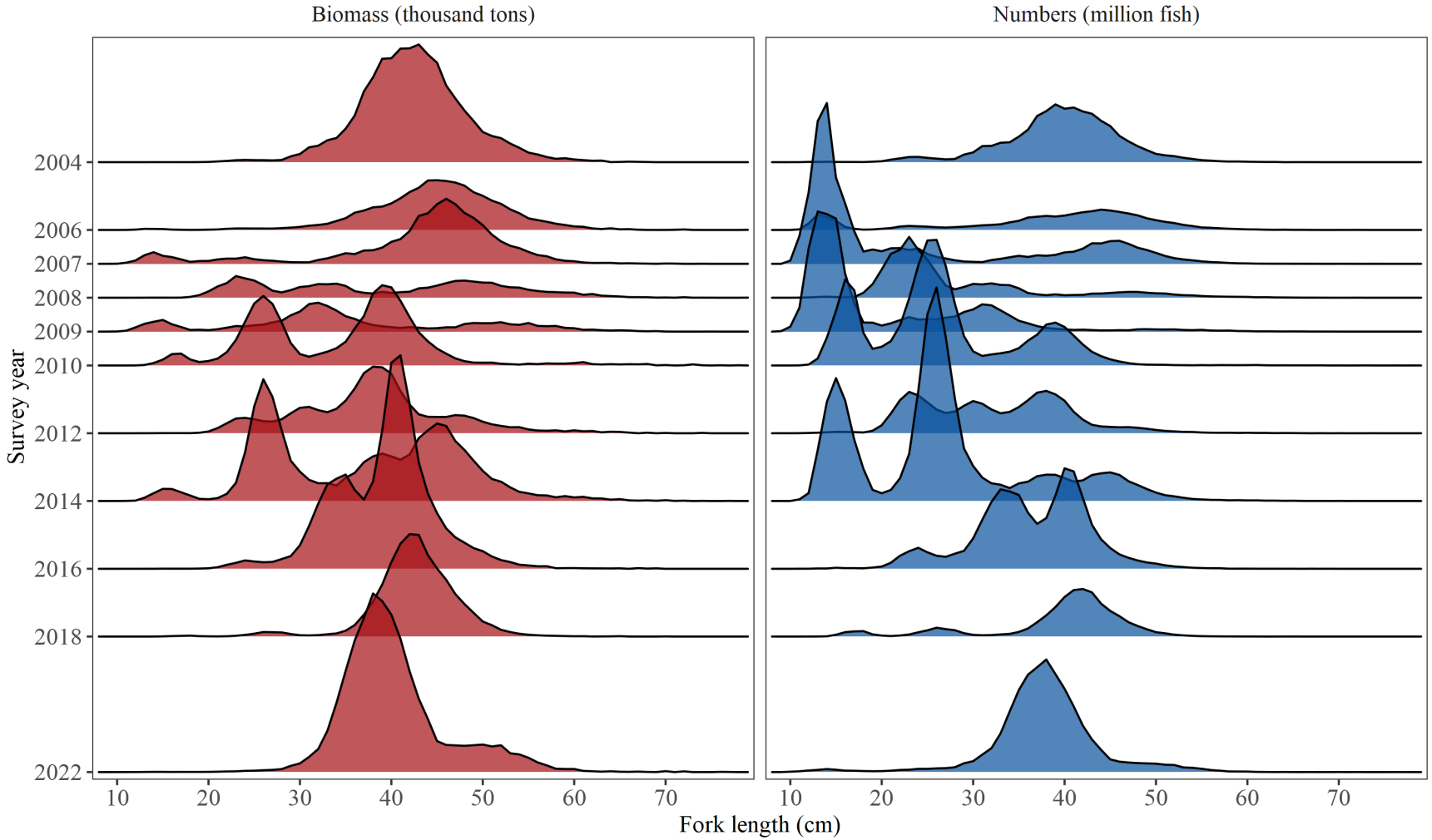

Figure 12. -- Time series of pollock population length composition by biomass (left panel) and numbers (right panel) from acoustic-trawl surveys of the eastern Bering Sea core area from 2004 to 2022. The scale is the same for all years pictured.

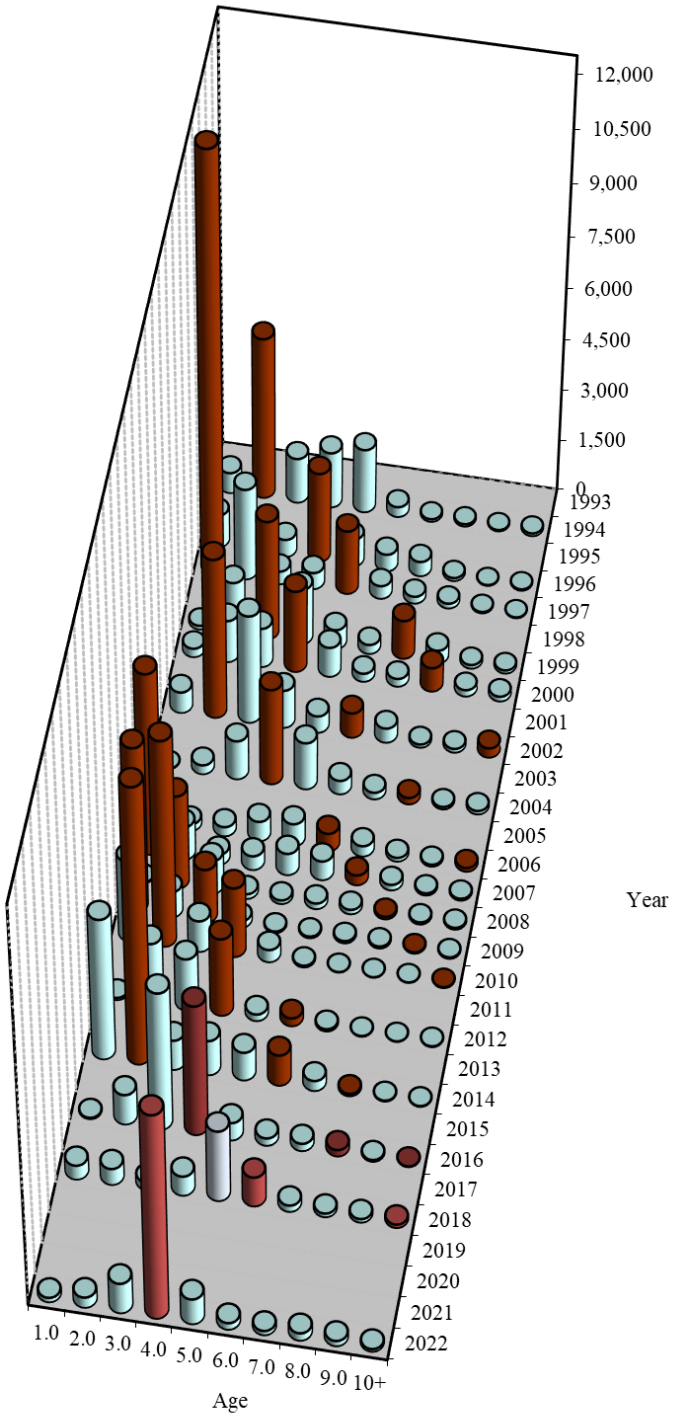

Figure 13. -- Historical numbers-at-age of walleye pollock between near surface and 0.5 m off bottom in the standard historical survey (core) area of the U.S. Exclusive Economic Zone (EEZ) for summer eastern Bering Sea shelf acoustic-trawl surveys between 1994 and 2022. Strong year classes are indicated with dark columns.

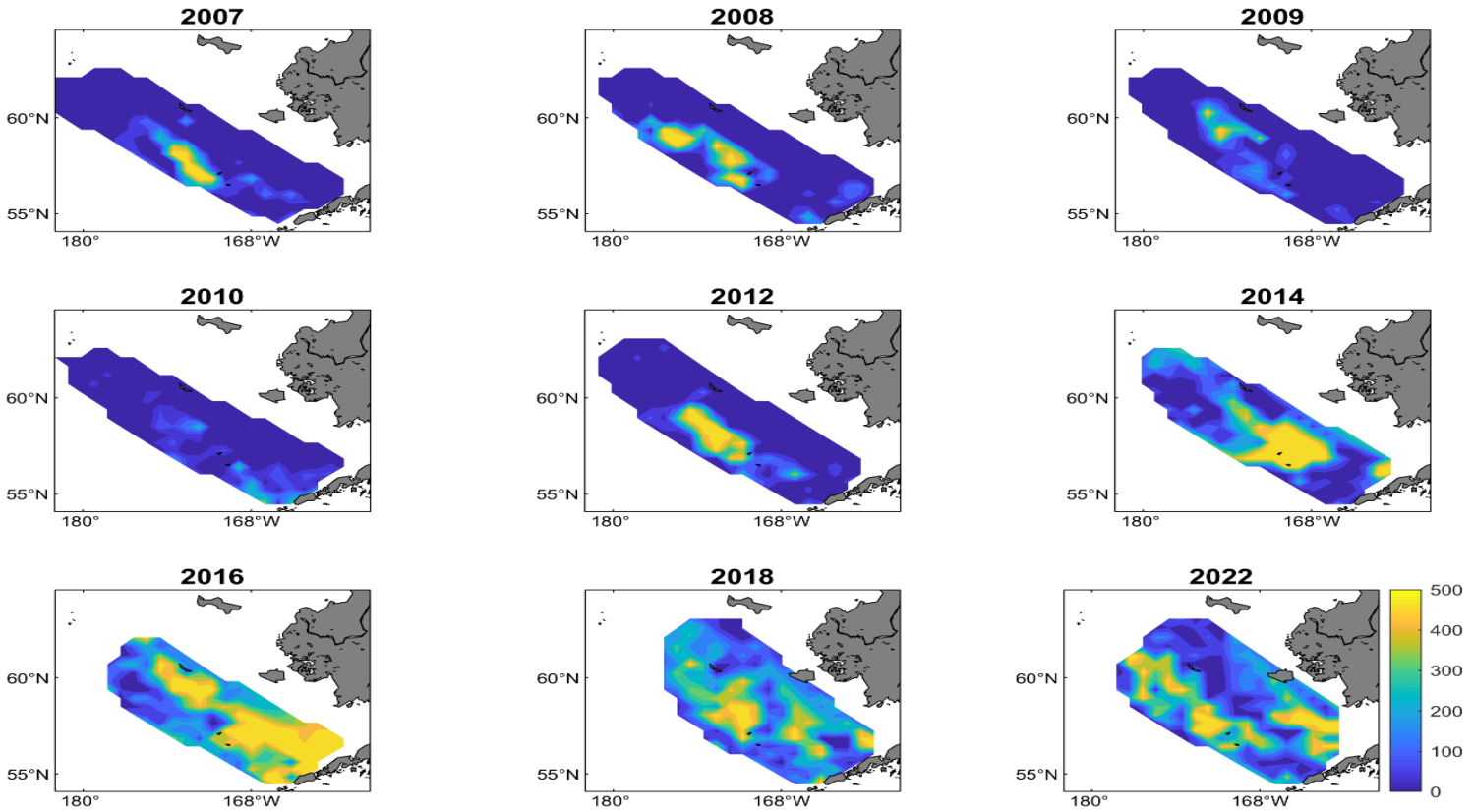

Figure 14. -- Backscatter attributed to a persistent non-walleye pollock, non-fish species mixture between near surface and 0.5 m off bottom, typically observed above the thermocline, in the U.S. Exclusive Economic Zone (EEZ) for summer eastern Bering Sea shelf acoustic-trawl surveys between 2007 and 2022.

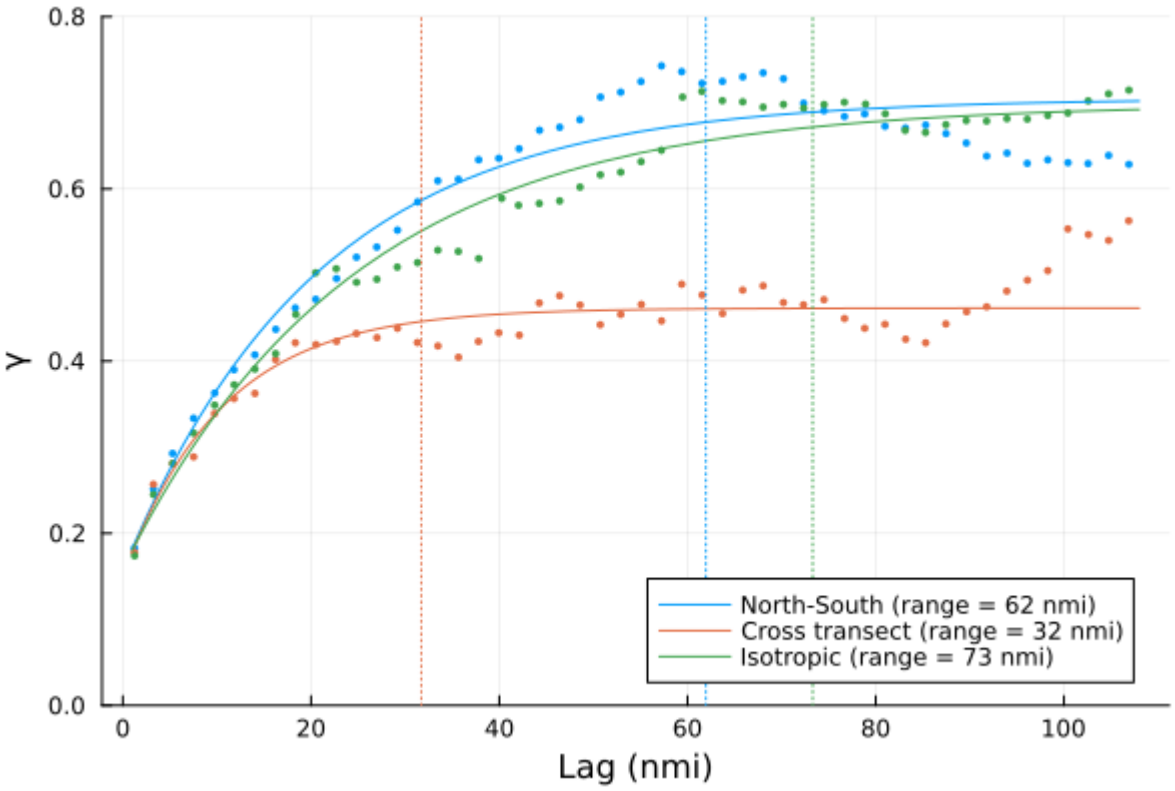

Figure 15. -- Empirical variograms (points) with fitted exponential models (solid lines) for the three directional analyses. Blue points and line show the variogram for the north-south direction, orange for the cross-shelf transect (144° true), and green for the overall, omnidirectional variogram. The variogram functions (γ) show that semivariance increases with lag distance, and then asymptotes as widely separated locations become decorrelated. Ranges (i.e., the decorrelation distances) for each variogram model are indicated in the legend and plotted as vertical dotted lines.

APPENDIX I. ITINERARY

Leg 1

31 May	Calibration in Captains Bay
2 June	Depart Dutch Harbor, AK. Transit to survey start area in Bristol Bay, eastern Bering Sea
3-15 June	Acoustic-trawl survey of the Bering Sea shelf. Transit to Unalaska Island, AK
16 June	Broadband data collection on the north side of Unalaska Island, AK
17 June	In port Dutch Harbor, AK

Leg 2

21 June	Transit to survey resume point
22 June - 8 July	Acoustic-trawl survey of the Bering Sea shelf
8-9 July	Transit to Unalaksa Island, AK, for a medical emergency
9-10 July	Calibration in Captains Bay
10 July	In port Dutch Harbor, AK

Leg 3

20-21 July	Transit to survey resume point
21-31 July	Acoustic-trawl survey of the Northern Extension
31 July - 3 Aug.	Cross transects over the Bering Sea shelf
3-4 Aug.	Transit to Unalaska Island, AK.
5 Aug.	Calibration in Captains Bay
5 Aug.	End of cruise. Dutch Harbor, AK

APPENDIX II. SCIENTIFIC PERSONNEL

Name	Position	Organization	Nation
	Leg 1 (2-17 June)		
Sarah Stienessen	Chief Scientist	AFSC	USA
Abigail McCarhty	Fishery Biologist	AFSC	USA
Nate Lauffenburger	Fishery Biologist	AFSC	USA
Scott Furnish	Info. Tech. Specialist	AFSC	USA
Sandy Parker-Stetter	Fishery Biologist	AFSC	USA
Matthew Phillips	Observer	AIS	USA
James Gossom	Observer	AIS	USA
	Leg 2 (21 June -10 July)		
Taina Honkalehto	Chief Scientist	AFSC	USA
Kresimir Williams	Fishery Biologist	AFSC	USA
Mike Levine	Info. Tech. Specialist	AFSC	USA
Matthew Phillips	Observer	AIS	USA
James Gossom	Observer	AIS	USA
Dereka Chargualaf	Fish Biologist	WCR	USA
Caroline Lawrence	Fish Biologist	AFSC	USA
	Leg 3 (20 July -5 August)		
Patrick Ressler	Chief Scientist	AFSC	USA
Rick Towler	Info. Tech. Specialist	AFSC	USA
Darin Jones	Fishery Biologist	AFSC	USA
Dave McGowen	Fishery Biologist	AFSC	USA
Denise McKelvey	Fishery Biologist	AFSC	USA
Matthew Phillips	Observer	AIS	USA
James Gossom	Observer	AIS	USA

AFSC	Alaska Fisheries Science Center, Seattle WA
AIS	AIS, Inc., New Bedford, MA
PCMSC	Pacific Coastal and Marine Science Center, Santa Cruz CA

APPENDIX III. ABUNDANCE CALCULATIONS

The abundance of target species was calculated by combining the echosounder measurements with size and species distributions from trawl catches and target strength (TS) to length relationships from the literature (see De Robertis et al. 2017b for details). The echosounder measures volume backscattering strength, which is integrated vertically to produce the nautical area scattering coefficient, s_A (units of m^2 nmi^{-2}; MacLennan et al. 2002). The backscatter from an individual fish of species s at-length l is referred to as its backscattering cross-section, $\sigma_{bs_{s,l}}$ (m^2), or in logarithmic terms as its target strength, $TS_{s,l}$ (dB re 1 m^2):

$$TS_{s,l} = 10\log_{10}\left(\sigma_{bs_{s,l}}\right) . \qquad \text{(Eq. } i\text{)}$$

The numbers of individuals of species s in length class l ($N_{s,l}$) captured in the nearest haul h were used to compute the proportion of acoustic backscatter associated with each species and length. First, the number of individuals in the catch were converted to a proportion ($P_{s.l,h}$):

$$P_{s,l,h} = \frac{N_{s,l,h}}{\sum_{s,l} N_{s,l,h}} , \quad \text{where} \sum_{s,l} P_{s,l,h} = 1 . \qquad \text{(Eq. } ii\text{)}$$

In analyses where trawl selectivity was considered, the selectivity-corrected numbers $N_{s_{corr},l,h}$ were used in place of $N_{s,l,h}$ in Eq. ii. This correction corrects the catch for trawl escapement. The corrected catch is that expected for an unselective sampling device. Refer to the main text for a description of the selectivity corrections applied.

The mean backscattering cross-section (an areal measure of acoustic scattering in m^2; MacLennan et al 2002) of species s of length class l is:

$$\sigma_{bs_{s,l}} = 10^{(0.1 \cdot TS_{s,l})} , \qquad \text{(Eq. } iii\text{)}$$

where TS is the target strength of species *s* at size *l* (Table 3).

The proportion of backscatter from species s of length class l in haul h ($PB_{s,l,h}$) is computed from the proportion of individuals of species s and length class l estimated from haul h ($P_{s,l,h}$) and their backscattering cross-section:

$$PB_{s,l,h} = \frac{P_{s,l,h} \cdot \sigma_{bs_{s,l}}}{\sum_{s,l}\left(P_{s,l,h} \cdot \sigma_{bs_{s,l}}\right)} . \qquad \text{(Eq. } iv\text{)}$$

The measured nautical area backscattering coefficient (s_A) at interval i was allocated to species s and length l as follows:

$$s_{A_{s,l,i}} = s_{A_i} \cdot PB_{s,l,h} , \qquad \text{(Eq. } v\text{)}$$

where haul h is the nearest haul within a stratum assigned to represent the species composition in a given 0.5 nmi along-track interval i. The nearest geographic haul was determined by using the great-circle distance to find the nearest trawl location (defined as the location where the net is at depth and begins to catch fish) out of the pool of hauls assigned to the same stratum (see above for details) closest to the start of interval i.

The abundance of species of length l in an area encompassing a series of transect intervals i was estimated from the area represented by that interval (A_i, nmi^2), the mean areal backscatter attributed to species s in given length/size class l ($s_{A_{s,l,i}}$, m^2 nmi^{-2}), and mean backscattering cross-section of species s at that size ($\sigma_{bs_{s,l}}$ m^2) as follows:

$$\text{Numbers-at-length } l\text{: } N_{s,l} = \sum_i \left(\frac{s_{A_{s,l,i}}}{4\pi\sigma_{bs_{s,l,i}}} \times A_i \right) \qquad \text{(Eq. } vi\text{)}$$

$$\text{Biomass-at-length } l\text{: } B_{s,l} = \sum_i \left(W_{s,l} \times N_{s,l,i} \right) \ , \qquad \text{(Eq. } vii\text{)}$$

where $W_{s,l}$ is the mean weight-at-length for species s in each 1-cm length l derived from length-weight regressions. A_i is the distance of the along-track interval i multiplied by the interval width. The inverval width is the sum of half the distance between the two directly adjacent transects. For a transect at the edge of an area, the interval width equals the distance betweewn the directly adjacent transect.

In the case of pollock, when five or more individuals were measured within a length interval, the mean weight-at-length was used. Otherwise (i.e., for length classes of pollock with < 5 weight measurements, or other species), weight-at-length was estimated using a linear regression of the natural log-transformed length-weight data (De Robertis and Williams 2008).

The abundance-at-age was computed from $Q_{s,l,j}$, the proportion of j-aged individuals of species s in length class l, and the abundance of that species and age class in each surveyed interval follows:

$$\text{Numbers-at-age } j\text{: } N_{s,j} = \sum_i \left(Q_{s,l,j} \times N_{s,l} \right) \qquad \text{(Eq. } viii\text{)}$$

$$\text{Biomass-at-age } j\text{: } B_{s,j} = \sum_i \left(Q_{s,l,j} \times B_{s,l} \right) \ . \qquad \text{(Eq. } ix\text{)}$$

Acting U.S. Secretary of Commerce
Jeremy Pelter

Acting Under Secretary of Commerce
for Oceans and Atmosphere
Nancy A. Hann

Acting Assistant Administrator,
National Marine Fisheries Service
Emily Menashes

February 2025

www.fisheries.noaa.gov

OFFICIAL BUSINESS

National Marine
Fisheries Service
Alaska Fisheries Science Center
7600 Sand Point Way N.E.
Seattle, WA 98115-6349